

WATER BALANCE AND EQUILIBRIUM EVAPOTRANSPIRATION

EVAPOTRANSPIRATION ESTIMATES  
FROM THE  
WATER BALANCE  
AND  
EQUILIBRIUM MODELS

BY

RICHARD GARTH WILSON, M.Sc.

A Thesis

Submitted to the School of Graduate Studies  
in Partial Fulfilment of the Requirements  
for the Degree  
Doctor of Philosophy

McMaster University

May 1971

DOCTOR OF PHILOSOPHY (1971)  
(Geography)

McMASTER UNIVERSITY  
Hamilton, Ontario.

TITLE: Evapotranspiration Estimates from the Water Balance  
and Equilibrium Models

AUTHOR: Richard Garth Wilson, B.Sc. (McGill University)

M.Sc. (McGill University)

SUPERVISOR: Professor W. R. Rouse

NUMBER OF PAGES: xi, 123

SCOPE AND CONTENTS:

This thesis examines the field performance of the water balance and equilibrium evapotranspiration models, and defines the environmental conditions for which they provided accurate estimates of water loss from a corn crop in Southern Ontario.

It is shown that the water balance model should be used only when surface runoff is measured and drainage is negligible. An error analysis indicated that soil moisture change could be estimated within 10 percent when measurements were conducted at six sites every eight days.

The equilibrium model predicted daily evapotranspiration within 6 percent when the latent heat exchange utilized between 65 and 80 percent of the available energy, indicating that the model can be applied within temperature limits of 17° and 32°C.

## ACKNOWLEDGEMENTS

This study comprises a part of a microclimatological research program being conducted at the Simcoe Horticultural Experiment Station at Simcoe, Ontario. I wish to express my gratitude to those who are affiliated with the program and to others who helped me during the course of the study.

Special thanks go to Dr. W. R. Rouse and Dr. J. A. Davies for their guidance and assistance during all phases of the work. Dr. Rouse gave invaluable assistance during the exhausting measurement program, and Dr. Davies introduced me to the concept of equilibrium evapotranspiration. I also wish to thank Dr. G. Collins, the Director of the Simcoe Horticultural Experiment Station for his co-operation during my field work.

Further acknowledgements go to Mr. J. H. McCaughey who helped with much of the field work, to Miss M. Gingras for her assistance with the typing, to Mr. H. Fritz for drawing the diagrams, and to the National Research Council of Canada for its continuous support during my studies.

I especially wish to thank my wife Susan who helped with the field observations, typed most of the thesis, and has given me encouragement throughout my university studies.

## TABLE OF CONTENTS

	Page
DESCRIPTIVE NOTE	ii
ACKNOWLEDGEMENTS	iii
TABLE OF CONTENTS	iv
LIST OF FIGURES	vii
LIST OF TABLES	x
LIST OF PLATES	xi
CHAPTER 1 OBJECTIVES AND APPROACH	1
1. Objectives	1
2. The Water Balance Model	1
3. The Equilibrium Model	2
4. Approach to the Problem	3
CHAPTER 2 THEORETICAL DEVELOPMENT OF THE WATER BALANCE, THE ENERGY BALANCE, AND EQUILIBRIUM EVAPOTRANSPIRATION	4
1. The Water Balance Model	4
2. The Energy Balance	7
3. The Equilibrium Model	16
CHAPTER 3 SITE, INSTRUMENTATION, AND EXPERIMENTAL PROCEDURE	25
1. Site	25
2. Measurements for the Water Balance	25
(i) Precipitation	25

TABLE OF CONTENTS (cont'd)

	Page
(ii) Soil moisture content	27
(iii) Drainage	36
3. Measurements for the Energy Balance	46
(i) Net radiation	46
(ii) Soil heat flux	47
(iii) Temperature gradients and wet-bulb depressions	50
4. Calculations for the Equilibrium Model	55
CHAPTER 4 ENERGY BALANCE COMPONENTS AND EVAPO- TRANSPIRATION ESTIMATES FROM THE WATER BALANCE MODEL	56
1. Energy Balance Regime	56
2. Water Balance Regime	61
3. Evapotranspiration Estimates from the Water Balance	64
(i) Accuracy of the estimates	64
(ii) Spatial variations in $\Delta S_m$	67
(iii) Error analysis of $\Delta S_m$ estimates	74
(iv) Evaluation of drainage and its effect on the water balance estimates of evapotranspiration	82
4. Significance of Results	92
CHAPTER 5 EVAPOTRANSPIRATION ESTIMATES FROM THE EQUILIBRIUM MODEL	93
1. Performance in Relation to Available Moisture	93
2. Performance in Relation to Wet-Bulb Depression Profiles	103

TABLE OF CONTENTS (cont'd)

	Page
3. Moisture and Temperature Limits	106
4. Significance of Results	111
CHAPTER 6 SUMMARY AND CONCLUSIONS	112
1. The Water Balance Model	112
2. The Equilibrium Model	114
REFERENCES	116

## LIST OF FIGURES

Number		Page
1	Illustration of the water balance of a vegetated plot of land	5
2	Graphical illustration of the natural evaporation process	17
3	Location of equipment at the Simcoe experimental site	26
4	Counting time errors at the 95% probability level	30
5	Neutron depth probe calibration	32
6	Neutron surface probe calibration	37
7	Arrangement of tensiometers	39
8	Illustration of pressure cell for measuring capillary conductivity of soil	43
9	Illustration of temperature and humidity measurement system	52
10	Variation of energy balance components during July 1969	57
11	Variation of daily Bowen Ratio values during July 1969	57
12	Trends of the ratios $G/R_n$ and $G_5/R_n$ on a daily basis during July 1969	59
13	Variation of energy balance components and equilibrium evapotranspiration on July 6, 1969	60
14	Variation of precipitation and soil moisture storage during July 1969	62

LIST OF FIGURES (cont'd)

Number		Page
15	Daily and 4-day values of $(P - \Delta Sm)$ during July 1969	63
16	Relationships between daily values of E from the energy balance and $(P - \Delta Sm)$ when the moisture content of the 25 cm surface layer was measured by (A) the gravimetric method and (B) the neutron surface probe	65
17	Relationships between 4-day totals of E from the energy balance and (A) mean values of $(P - \Delta Sm)$ and (B) individual values of $(P - \Delta Sm)$	66
18	Profiles of hydraulic head at sites 1 and 5 on selected days during July 1969	70
19	Soil moisture content profiles at sites 1 and 5 on selected days during July 1969	83
20	Moisture characteristic for 140 cm depth at site 5	85
21	Generalized moisture characteristics for various depths at site 5	87
22	Moisture characteristics at 120 cm, 140 cm, and 160 cm depths using data from all sites	88
23	Capillary conductivity values for the 140 cm depth determined by various methods	90
24	Relationship between daily values of E from the energy balance and $E_{EQ}$ from the equilibrium model	95
25	Variation of energy balance components and equilibrium evapotranspiration on July 18, 1969	97
26	Variation of soil moisture content in the 0-25 cm surface layer during July 1969	99

LIST OF FIGURES (cont'd)

Number		Page
27	Variation of energy balance components and equilibrium evapotranspiration on July 12, 1969	101
28	Variation of energy balance components and equilibrium evapotranspiration on July 15, 1969	102
29	Wet-bulb depression profiles on four days during July 1969	105
30	Relationship between the ratio $E/E_{EQ}$ and the ratio $LE/(R_n - G)$ for daily periods	107
31	Variation of the factor $S/(S + \gamma)$ with temperature	109

## LIST OF TABLES

Number		Page
1	Regression and correlation constants for neutron probe calibrations of the form $\theta$ (volume fraction) = $a + bR$ (cpm)	33
2	Soil densities ( $\text{g cm}^{-3}$ ) at each site	35
3	Precipitation (P) and soil moisture change ( $\Delta S_m$ ) in mm at six sites from July 1 to July 25	68
4	Correlation coefficient matrix for (P - $\Delta S_m$ ) values	69
5	Soil moisture change (mm) in the 0-25 cm layer	71
6	Soil moisture change (mm) in the 25-80 cm layer	72
7	Soil moisture change (mm) in the 80-140 cm layer	73
8	Summary of absolute errors in $\Delta S_m$ (mm)	79
9	Summary of percentage errors in $\Delta S_m$	79
10	Mean hydraulic gradients at the six sites	86
11	Regression and correlation constants for the relationship between E and $E_{EQ}$ of the form $E = a + bE_{EQ}$ ( $\text{mm day}^{-1}$ )	94

LIST OF PLATES

Number

Page

1

Temperature and humidity mast

51

## CHAPTER 1

### OBJECTIVES AND APPROACH

#### 1. Objectives

In recent years there has been a sustained effort to obtain reliable estimates of evapotranspiration using simple methods which require a minimum of easily-obtained measurements. It is the object of this thesis to examine in detail two approaches which are basically simple both in theory and in application, and to comment critically on the conditions under which they are applicable. The two methods are derived from principles of the conservation of water and the conservation of energy and are referred to as the water balance model and the equilibrium model respectively.

#### 2. The Water Balance Model

The water balance model treats evapotranspiration as a residual after a balance has been made between the water input to a plant-covered soil block by precipitation, dewfall and/or irrigation, and changes in water storage in the soil block. Storage changes account for lateral and vertical movement of water into and out of the soil block,

and evapotranspiration. The model is attractive because the two major components of the water balance, precipitation and soil moisture storage change, can be easily and quickly measured. Evidence of the reliability of this approach is conflicting. For example, Bowman and King (1965), in calculating evapotranspiration over weekly intervals in non-irrigated conditions, found that accumulated totals of evapotranspiration were in good agreement with those measured with a lysimeter. In contrast, van Bavel et al. (1968a), using measurements from an irrigated field for 4-day intervals, found that the estimates were in error by as much as 30 percent. Since the water balance model is used widely in river basin hydrology studies there is a need to develop restraints within which the model is applicable.

### 3. The Equilibrium Model

The theory of the equilibrium evapotranspiration model was first presented by Slatyer and McIlroy (1961) and is usually attributed to the second author. Evapotranspiration is calculated from the rate of latent heat flow from the surface into the atmosphere, which is derived as a function of the heat energy available for evaporation. As in the case of the water balance model, the equilibrium model has the desirable attributes that it requires few and simple measurements. In studies by Monteith (1965), Tanner

and Fuchs (1968), and Pruitt and Lourence (1968) the model was considered to apply only in a saturated atmosphere. More recently, however, Denmead and McIlroy (1970) have shown that it also applies to non-saturated conditions. Due to the simplicity and theoretical soundness of the equilibrium model it is important to determine the environmental conditions under which it can be applied.

#### 4. Approach to the Problem

The accuracy of evapotranspiration estimates from the two models has been determined by comparison to calculations made from energy balance measurements. The experiments were conducted at the Simcoe Horticultural Experiment Station in Southern Ontario in a corn crop growing in sandy loam soil. The experimental program spanned twenty five days in July 1969 and the frequency of measurements allowed comparisons to be made for various time periods, for various conditions of available moisture and for a variety of temperature conditions.

## CHAPTER 2

### THEORETICAL DEVELOPMENT OF THE WATER BALANCE, THE ENERGY BALANCE, AND EQUILIBRIUM EVAPOTRANSPIRATION

#### 1. The Water Balance Model

The water balance of a vegetated soil plot involves six processes which are illustrated in Fig. 1 and are expressed in the water balance equation

$$E = P - \Delta S_m - V_z - S_r - L_s \quad (1)$$

where  $E$  = evapotranspiration (cm),

$P$  = precipitation (cm),

$\Delta S_m$  = soil moisture storage change over an interval  
of time (cm),

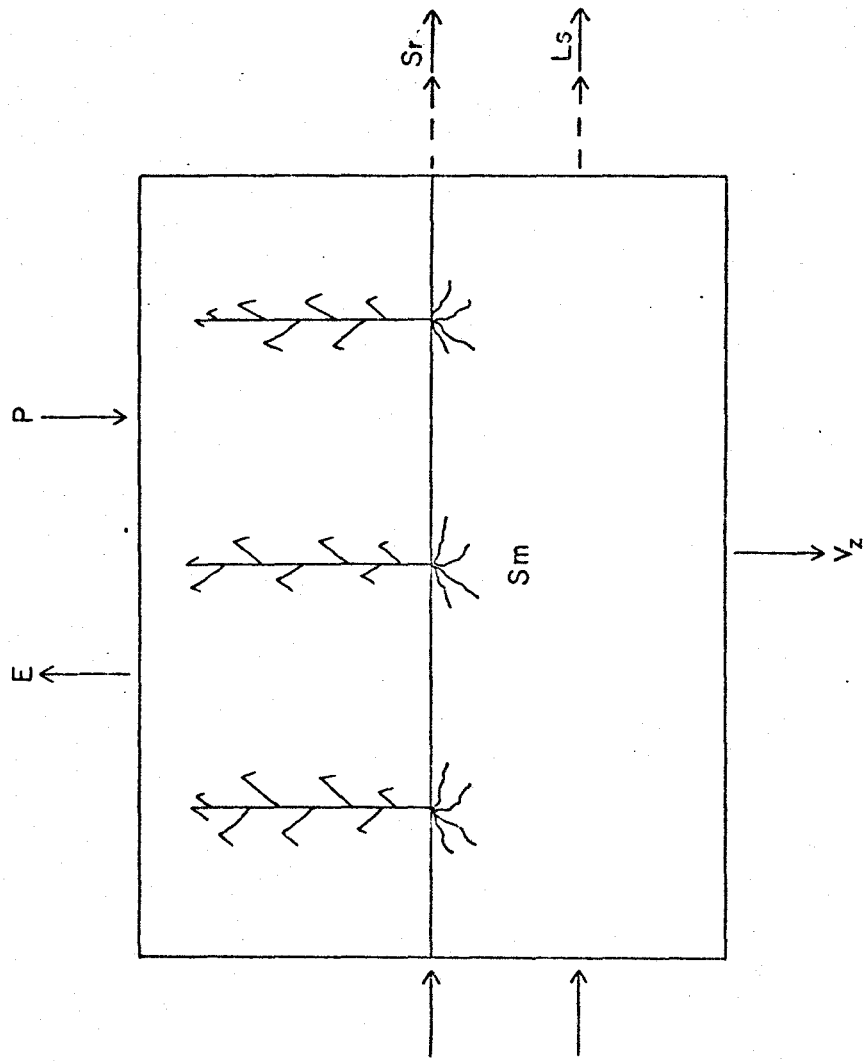
$V_z$  = drainage at the terminal depth of measurements  
(cm),

$S_r$  = the net water loss due to surface runoff (cm),  
and

$L_s$  = the net water loss due to lateral subsurface  
water movement (cm).

In practical applications, horizontal surface and subsurface water losses are frequently neglected for small plots of land.

FIGURE I  
ILLUSTRATION OF THE WATER BALANCE OF A VEGETATED PLOT OF LAND



The assumption of no surface runoff is generally valid for situations where land is flat, the infiltration capacity of the soil is high, and there are no intense rainstorms. Surface runoff may occur even on very porous soils during intense rains as shown later in this report.

Rouse (1970) found that  $L_s$  was negligible in the sandy loam soil at Simcoe, even in the presence of large horizontal moisture gradients.

By neglecting  $S_r$  and  $L_s$ , the water balance equation reduces to

$$E = P - \Delta S_m - V_z \quad (2)$$

The total depth of water present in the soil profile ( $S_m$ ) at any time is given by

$$S_m = \int_0^Z \theta \, dz \quad (3)$$

where  $\theta$  = volumetric soil moisture content, and

$Z$  = the terminal depth of measurements (cm).

$\Delta S_m$  is obtained by subtracting successive values of  $S_m$ .

The amount of drainage out of the plot can be determined by an hydraulic gradient method in which

$$V_z = - \int_{t_1}^{t_2} k_z \frac{d\phi}{dz} \, dt \quad (4)$$

where  $k_z$  = the capillary conductivity of the soil at depth  $Z$  ( $\text{cm hour}^{-1}$ ),  
 $\phi$  = the total water potential, or hydraulic head (cm of water),  
 $d\phi/dZ$  = the hydraulic gradient, and  
 $t$  = time (hours).

$k_z$  increases with increasing moisture content for any given soil.

In an unsaturated soil under isothermal conditions  $\phi$  can be expressed as

$$\phi = -(\psi + Z) \quad (5)$$

where  $\psi$  = matric suction (cm of water).

The negative sign denotes a pressure which is less than atmospheric.

## 2. The Energy Balance

The process of evapotranspiration provides the link between the water and energy balances of the land surface. In order to sustain a flux of water vapour from the surface to the atmosphere, heat must be supplied to convert the liquid water to vapour. Thus, it is possible to obtain a measure of the amount of water transferred to the atmosphere by assessing the associated heat flux. This is the

principle of the energy balance method of measuring evapotranspiration. The balance of all gains and losses of energy for an evapotranspiring surface is given by

$$R_n + \text{div. } H + \text{div. } LE = LE + H + G + A + Q_b + Q_a \quad (6)$$

where

- $R_n$  = the net radiation flux,
- $H$  = the sensible heat flux,
- $LE$  = the latent heat flux,
- $L$  = the latent heat of vapourization of water (586 cal  $g^{-1}$  at 20°C),
- $E$  = the evapotranspiration rate (cm  $min^{-1}$ ),
- div.  $H$  = horizontal divergence of sensible heat,
- div.  $LE$  = horizontal divergence of latent heat,
- $G$  = the soil heat flux,
- $A$  = the amount of energy stored by net photosynthesis,
- $Q_b$  = the net change in heat storage in the biomass, and
- $Q_a$  = the net change in heat storage in the air within the plant canopy.

All terms in eq. (6) are expressed in units of cal  $cm^{-2} min^{-1}$  or cal  $cm^{-2} day^{-1}$  in this report.

It must be emphasized that this complete balance equation is applicable to any three-dimensional surface and

accounts for horizontal as well as vertical energy fluxes. In practice, the balance must be simplified because of the difficulty of measuring  $\text{div. } H$  and  $\text{div. } LE$ . It is customary, therefore, to consider the balance at a location where the vertical fluxes are constant with height so that the divergence terms can be safely neglected. This condition of flux constancy with height is the characteristic which defines the atmospheric surface boundary layer. The depth of this layer increases with down wind distance from the edge of the surface. Consequently it is common practice to choose a measurement site in the midst of a large uniform surface so that only the vertical fluxes and storage terms need to be considered.

The terms  $Q_a$ ,  $Q_b$ , and  $A$  are normally small enough to be neglected for hourly and daily totals. A change of energy storage in the air is indicated by an increase or decrease in the amounts of sensible and latent heat in the air layer between the ground and the top of the vegetation, and can be expressed as

$$Q_a = 0 \int^Z \rho_a c_p \frac{dT}{dt} dz + 0 \int^Z \frac{L \epsilon}{R'T} \frac{de}{dt} dz \quad (7)$$

where  $\rho_a$  = air density ( $\text{g cm}^{-3}$ ),

$c_p$  = the specific heat of air at constant pressure  
( $\text{cal g}^{-1} \text{deg}^{-1}$ ),

- $T$  = air temperature ( $^{\circ}\text{K}$ ),  
 $Z$  = height (cm),  
 $\epsilon$  = the ratio of the molecular weights of water and air,  
 $R'$  = the specific gas constant for air ( $\text{mbar cm}^3 \text{g}^{-1} \text{deg}^{-1}$ ), and  
 $e$  = water vapour pressure in the air (mbar).

In an extreme case, a 100 cm air layer might experience a temperature change of  $10^{\circ}\text{K}$  and a 1 mbar vapour pressure change over a period of an hour. This would indicate a change in the sensible heat content equivalent to an energy flux of  $0.005 \text{ cal cm}^{-2} \text{ min}^{-1}$ . Assuming a mean air temperature of  $25^{\circ}\text{C}$ , there would be a change in the latent heat content equivalent to a flux of  $0.0007 \text{ cal cm}^{-2} \text{ min}^{-1}$ . The combined total for energy storage in the air would then be less than  $0.006 \text{ cal cm}^{-2} \text{ min}^{-1}$ . This flux would usually represent less than 1 percent of the net radiation during daytime hours, except for brief periods near sunrise and sunset.

It can also be shown that changes of the heat storage in the biomass are usually negligible. In this case the change of heat storage is given by

$$Q_b = \int_0^Z \rho_b c_b \frac{dT_b}{dt} dz \quad (8)$$

where  $\rho_b$  = the density of the biomass ( $\text{g cm}^{-3}$ ),  
 $c_b$  = the specific heat of the biomass ( $\text{cal g}^{-1}$   
 $\text{deg}^{-1}$ ), and  
 $T_b$  = the temperature of the biomass ( $^{\circ}\text{C}$ ).

Consider a simplified corn crop. Assume that the plants are 100 cm tall, each with an area of  $1 \text{ cm}^2$ , and are separated by 15 cm in rows which are 90 cm apart. To simplify the calculation, it is assumed that the plants consist entirely of water and that an extreme air temperature change of  $10^{\circ}\text{C hr}^{-1}$  also occurs in the plants. In this situation, the change in heat storage in the plants would represent a heat flux of only  $0.012 \text{ cal cm}^{-2} \text{ min}^{-1}$ . This value is larger than an actual flux would be for real plants but it is still negligible except for brief periods near sunrise and sunset. When considering daily totals of the energy budget,  $Q_a$  and  $Q_b$  can be completely neglected since storage gains during the morning hours are cancelled by losses in the afternoon period.

In most cases net photosynthesis is considered to use less than 5 percent of the net radiation (Yocum et al., 1964; Knoerr, 1965) but peak rates of 10 percent have been observed for early morning and late afternoon hours (Lemon, 1960). Since maximum evapotranspiration occurs at mid-day, the absolute error resulting from neglect of

the photosynthesis term will be small for most hourly values and for daily totals of the vapour flux. By omitting  $Q_b$ ,  $Q_a$ , and  $A$ , and considering the energy balance within the boundary layer, eq. (6) can be reduced to

$$R_n = LE + H + G \quad . \quad (9)$$

Both  $R_n$  and  $G$  are readily measured but there is no simple method of measuring  $H$ . However, it is possible to solve for  $LE$  by using the ratio  $H/LE$ . Rearranging eq. (9) and dividing by  $LE$  gives

$$LE = \frac{R_n - G}{1 + \frac{H}{LE}} \quad . \quad (10)$$

From mass transfer theory,

$$H = - \rho_a c_p K_H \frac{dT}{dz} \quad (11)$$

and

$$LE = - \frac{\rho_a \epsilon L}{p} K_w \frac{de}{dz} \quad (12)$$

where  $K_H$  = the eddy diffusivity for sensible heat ( $\text{cm}^2 \text{sec}^{-1}$ ),

$K_w$  = the eddy diffusivity for water vapour ( $\text{cm}^2 \text{sec}^{-1}$ ),

$p$  = atmospheric pressure (mbar), and  
 $Z$  = height (cm).

Dividing eq. (11) by eq. (12) gives

$$\frac{H}{LE} = \frac{c_p p}{L \epsilon} \frac{K_H}{K_W} \frac{dT/dZ}{de/dZ} \quad (13)$$

In normal practice  $dT/dZ$  and  $de/dZ$  can be defined as finite gradients  $\Delta T/\Delta Z$  and  $\Delta e/\Delta Z$ . If  $\Delta T$  and  $\Delta e$  are measured at the same heights eq. (13) becomes

$$\frac{H}{LE} = \frac{c_p p}{L \epsilon} \frac{K_H}{K_W} \frac{\Delta T}{\Delta e} \quad (14)$$

The term  $c_p p/L \epsilon$  is known as the psychrometric constant,  $\gamma$  ( $0.66 \text{ mbar } ^\circ\text{C}^{-1}$ ), and  $H/LE$  is known as the Bowen Ratio,  $\beta$ , (Bowen, 1926) giving

$$\beta = \gamma \frac{K_H}{K_W} \frac{\Delta T}{\Delta e} \quad (15)$$

Further simplification follows if it is assumed that  $K_H = K_W$ . Recent work by Swinbank and Dyer (1967) and Dyer (1967) has shown that this assumption is valid for a wide range of atmospheric stability. Hence it is possible

to reduce eq. (10) to

$$LE = \frac{R_n - G}{1 + \gamma \frac{\Delta T}{\Delta e}} \quad (16)$$

The temperature difference,  $\Delta T$ , can be measured directly but  $\Delta e$  must be calculated from psychrometric formulae which employ the wet-bulb temperature of the air. Atmospheric vapour pressure is calculated from the psychrometric formula

$$e = e_s - A' p (1 + 0.0015 T_W) (T - T_W) \quad (17)$$

where  $e_s$  = the saturation vapour pressure at  $T_W$ ,

$$A' = 0.000660 \text{ (}^\circ\text{C}^{-2}\text{)}$$

$T$  = air temperature ( $^\circ\text{C}$ ), and

$T_W$  = wet-bulb temperature ( $^\circ\text{C}$ ).

To simplify eq. (17) ,

$$\text{let } \gamma = A' p (1 + 0.00115 T_W) , \quad (18)$$

$$\text{and } D = T - T_W , \quad (19)$$

$$\text{so that } e = e_s - \gamma D \quad (20)$$

where  $D$  = the wet-bulb depression ( $^\circ\text{C}$ ).

Since normal atmospheric pressures at the earth's surface deviate only slightly from 1000 mbar, and since the correction for the wet-bulb temperature in eq. (18) is small, it is usually assumed that  $\gamma$  is constant at a value of  $0.66 \text{ mbar } ^\circ\text{C}^{-1}$ .

The accepted formulation of  $e_s$  was originally presented by Goff and Gratch (1946), but it is extremely complicated and is rarely used. A simplified approach by which  $\Delta e$  can be calculated directly was presented by Dilley (1968) who showed that by differentiating eq. (17) with respect to height, and retaining only the significant terms, the vapour pressure gradient can be written in finite difference form as

$$\frac{\Delta e}{\Delta Z} = (S + \gamma) \frac{\Delta T_W}{\Delta Z} - \gamma \frac{\Delta T}{\Delta Z} \quad (21)$$

where  $S$  = the slope of the saturation vapour pressure-temperature relationship at the mean wet-bulb temperature ( $\text{mbar deg}^{-1}$ ).

If the dry-bulb and wet-bulb temperatures are measured at the same heights,

$$\Delta e = (S + \gamma) T_W - \gamma \Delta T \quad (22)$$

Dilley showed that the value of S could be calculated accurately by taking the derivative of Tetens' (1930) approximation to the saturation vapour pressure.

The Tetens equation gives

$$e_s \approx 6.1078 \exp \frac{17.269 T_W}{T_W + 237.30} \quad (23)$$

and differentiation with respect to temperature gives

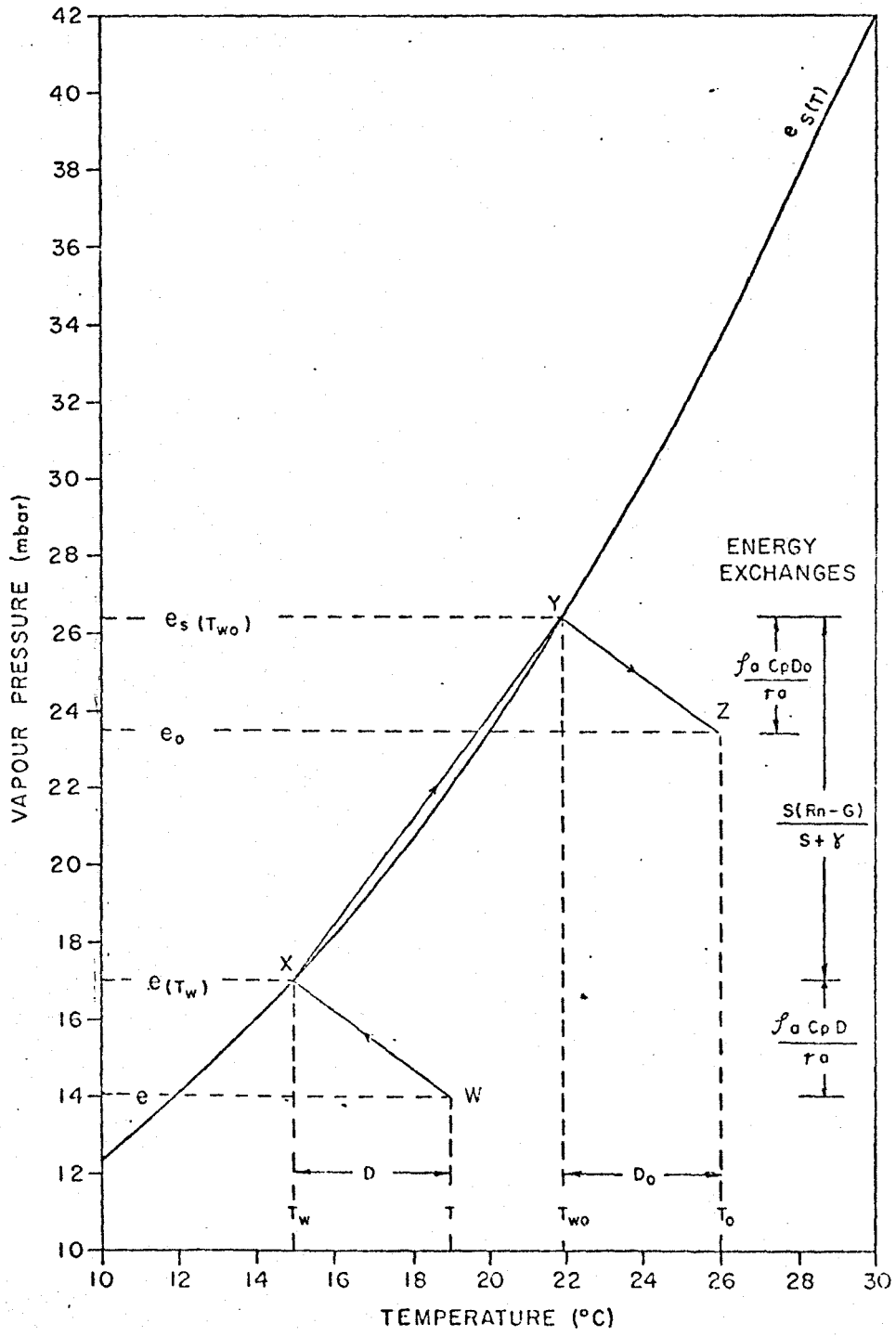
$$S = \frac{de_s}{dT_W} \approx \frac{25,029}{(T_W + 237.30)^2} \exp \frac{17.269 T_W}{T_W + 237.30} \quad (24)$$

Values of S calculated from eq. (24) agree within 0.1 percent with values determined from the Goff and Gratch equation over the temperature range 0°C to 50°C.

### 3. The Equilibrium Model

The process of natural evaporation can be described very simply by examining the energy exchanges which occur in an isolated parcel of air. This approach was presented by Monteith (1965) and a slightly modified version is illustrated in Fig. 2. A parcel of unsaturated air which is isolated from its surroundings has a temperature, T, and a vapour pressure, e. The state of this air is

FIGURE 2  
 GRAPHICAL ILLUSTRATION OF THE NATURAL  
 EVAPORATION PROCESS



signified by point W in Fig. 2. When the air is isolated from external sources of heat, evaporation of a small amount of liquid water in the parcel results in an increase in the vapour pressure and a corresponding decrease in the air temperature. Evaporation will stop when the air becomes saturated at the wet-bulb temperature,  $T_W$ , with the vapour pressure at the saturated level,  $e_s(T_W)$ . The condition of the saturated air is given by point X. The amount of energy expended on evaporation is equal to the increase in the latent heat content of the air, which must equal the decrease in the sensible heat content. For a unit volume, the latter is calculated as the product of the temperature decrease,  $(T - T_W)$ , and the heat capacity of the air,  $\rho_a c_p$ . By defining  $r_a$  as the time in which  $1 \text{ cm}^3$  of air exchanges heat with  $1 \text{ cm}^2$  of the water surface the latent heat flux during the saturation process,  $LE_1$ , can be written as

$$LE_1 = \frac{\rho_a c_p (T - T_W)}{r_a} = \frac{\rho_a c_p D}{r_a} \quad (25)$$

Evaporation will continue only if there is an addition of heat to the parcel of air. The amount of energy available to increase the heat content of the air

is given by  $(R_n - G)$  and the addition of this heat to the parcel of air will result in both an increase of the sensible heat content, thereby increasing the air temperature, and an increase of the latent heat content, with a corresponding increase in the vapour pressure. Since the air is saturated, small changes of temperature,  $dT_w$ , and vapour pressure,  $de_s$ , are related by

$$S dT_w = de_s \quad . \quad (26)$$

Brunt (1934) showed that small changes in temperature and vapour pressure may be related to the corresponding changes in the sensible heat content,  $dQ_H$ , and latent heat content,  $dQ_L$ , by

$$\frac{de}{dQ_L} = \frac{\gamma dT}{dQ_H} \quad . \quad (27)$$

Rearrangement of eq. (27) to consider the saturated case gives

$$\frac{de_s}{dT_w} dQ_H = \gamma dQ_L \quad (28)$$

and from eq. (26) and eq. (28),

$$S dQ_H = \gamma dQ_L \quad . \quad (29)$$

Adding and subtracting  $S dQ_L$  on the right hand side of eq. (29) and rearranging terms gives

$$S dQ_H = (S + \gamma) dQ_L - S dQ_L \quad (30)$$

and hence

$$dQ_L = \frac{S(dQ_H + dQ_L)}{S + \gamma} \quad . \quad (31)$$

The quantity  $dQ_L$  for unit time is equal to the latent heat flux,  $LE_2$ , during the saturated portion of the evaporation process so that

$$LE_2 = \frac{S(dQ_H + dQ_L)}{S + \gamma} \quad . \quad (32)$$

The increase in the heat content of the air in unit time is equal to  $(R_n - G)$ , so that

$$LE_2 = \frac{S(R_n - G)}{S + \gamma} \quad . \quad (33)$$

The parcel of air can be represented now by point Y in Fig. 2, which corresponds to the wet-bulb temperature of the air at the evaporating surface. If the air at the surface is not saturated, its condition can be represented by point Z. To reach this point from Y, latent heat must be released from the air at a rate

$$-LE_3 = \frac{\rho_a c_p D_o}{r_a} \quad (34)$$

where  $D_o$  = the wet-bulb depression in the air at the surface ( $^{\circ}\text{C}$ ).

The total latent heat flux, LE, for the path W to Z is the sum of the three components, which may be written as

$$LE = \frac{S(R_n - G)}{S + \gamma} + \frac{\rho_a c_p (D - D_o)}{r_a} \quad (35)$$

This equation was presented by Slatyer and McIlroy (1961). The value of S should be determined at the mean of the wet-bulb temperatures in the air and at the surface. However, temperatures at an evapotranspiring surface are difficult to measure accurately, particularly in the case of a plant canopy, so an approximation is required. In many daytime situations the difference between the two wet-bulb temperatures will be larger than the wet-bulb depression in the

overlying air. Thus the dry-bulb temperature of the air will lie between the two wet-bulb temperatures as shown in Fig. 2, making it possible to approximate the true value of  $S$  by the value at air temperature.

The term  $r_a$  is known as the aerodynamic resistance to the diffusion of water vapour, and is determined from the wind speed above the evapotranspiring surface and from the aerodynamic properties of that surface.

Eq. (35) is impractical for general use because of the difficulty of measuring  $D_o$ , but it is instructive because it separates the basic energy sources. The first term on the right hand side represents the net amount of radiant energy expended on evapotranspiration and the second term represents the energy used from the atmosphere for this purpose. It is the second term which is principally responsible for evapotranspiration differences between surfaces of different wetness. When a surface is wet or moist, the air close to it is saturated ( $D_o = 0$ ). This is the potential evapotranspiration condition which is considered in the Penman (1948) model. However, when the water supply to the surface is restricted  $D_o$  acquires a finite value and the actual evapotranspiration rate will be less than the potential. Recent evapotranspiration model developments by Monteith (1965), Tanner and Fuchs (1968) and Fuchs et al. (1969) have in fact been attempts

to eliminate  $D_0$  in favour of other parameters which are more easily measured or estimated. Slatyer and McIlroy (1961) considered the special and apparently limited case when the two depressions are equal, thereby eliminating the atmospheric term. This reduces eq. (35) to

$$LE = \frac{S(R_n - G)}{S + \gamma} \quad (36)$$

In this case the evapotranspiration rate is determined by the available radiant energy and the air temperature, with the Bowen Ratio equal to  $\gamma/S$ .

Monteith (1965) and Tanner and Fuchs (1968) have drawn attention to the fact that eq. (36) describes the evapotranspiration which would occur in a saturated atmosphere. This is the simplest case in which the depressions are equal, because both are equal to zero. However, it is possible that the depressions might have finite values and still be equal or nearly equal, in which case eq. (36) would remain valid or stand as a good approximation. Slatyer and McIlroy (1961) considered that equality of the depressions occurred when the surface and the overlying air had adjusted to one another, and suggested that the condition described by eq. (36) should be referred to as "equilibrium" evapotranspiration. This term will be used

hereafter and the rate of water loss by this process will be signified by  $E_{EQ}$ .

## CHAPTER 3

### SITE, INSTRUMENTATION, AND EXPERIMENTAL PROCEDURE

#### 1. Site

The research was conducted at the Horticultural Experiment Station at Simcoe in Southern Ontario during July 1969. Observations were made on a flat, rectangular (210 x 120 m) plot of sweet corn (*Zea Mays*: horticultural variety Seneca Chief). The corn plants were approximately 20 cm high when measurements were begun on July 1 and had reached a height of 105 cm on July 25 when measurements were terminated. The soil in this area is Caledon sandy loam to a depth of 45 cm. It is underlain by a very coarse sand to a depth of 200 cm at which point a heavy clay is encountered. Fig. 3 shows the measurement locations in the field.

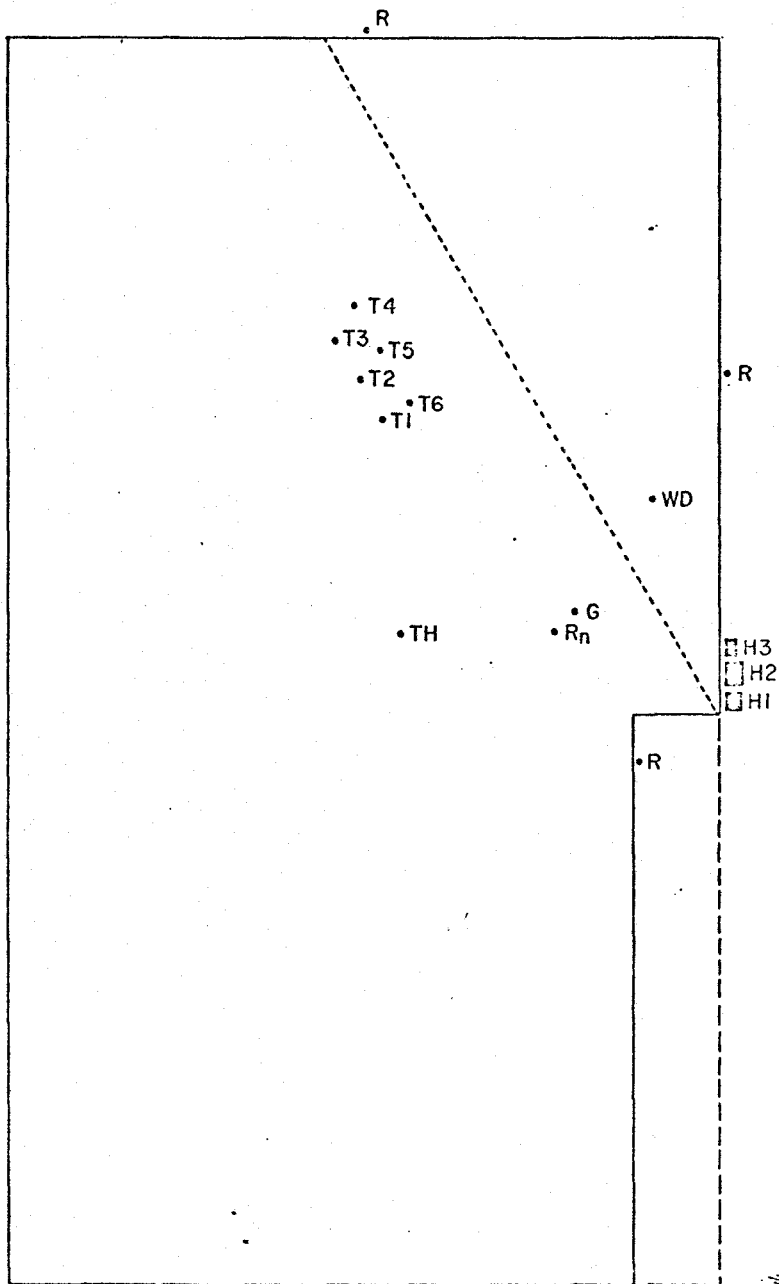
#### 2. Measurements for the Water Balance

##### (i) Precipitation

Precipitation was measured at three locations around the edge of the field with 5-inch diameter Casella raingauges. Measurements were averaged to give the mean rainfall for the field.

FIGURE 3

LOCATION OF EQUIPMENT AT THE SIMCOE EXPERIMENTAL SITE



- R - Rain Gauge
- T - Access Tube
- TH - Temperature and Humidity Mast
- H - Recording Hut
- R<sub>n</sub> - Net Radiometer
- G - Soil Heat Flux
- WD - Wind Dir. Vane
- Row Orientation

10 m



(ii) Soil moisture content

Volumetric soil moisture was measured with neutron moderation equipment. The instrumentation includes a probe, containing a source of high-energy (fast) neutrons and a detector of low-energy (slow) neutrons, and a scaler to count the number of slow neutrons detected in a certain time interval. Two types of probe were used: a depth probe which is lowered down an access tube to any desired soil depth, and a surface probe which is placed on a smooth soil surface. This equipment provides an indirect method of measuring moisture content. Fast neutrons emitted from the source into the soil are slowed by elastic collisions with other particles. The moderation by hydrogen nuclei, present mainly in the form of water, is much more efficient than that of other elements in the soil. Consequently, the density of the resultant cloud of slow neutrons is a function of the volumetric soil moisture. The measurement procedure entails obtaining a count rate (counts per minute, cpm) which can then be converted directly into volumetric moisture. Before conversion the count rate is corrected for background count and coincidence loss. Background counts are due to external sources of radioactivity and serve to increase the observed count rates. The background rate is measured in an access tube above the ground and is subtracted from the observed rates measured in the soil.

Coincidence loss is caused by radiation pulses arriving too rapidly to register separate counts, thus causing an underestimate of the true rate. The true count rate,  $R$ , is calculated from an equation presented by Washtell and Hewitt (1965) in which

$$R = \frac{r}{1-rt'} \quad (37)$$

where  $r$  = the observed rate (cpm), and

$t'$  = the resolution time of the equipment (min).

The counting time for a single probe reading is directly related to the accuracy of the measurement because the radioactive source decays in a random manner. This causes variations within a series of measurements at a fixed location. Bell and Eeles (1967) expressed the maximum acceptable error,  $\epsilon_I$ , in terms of the minimum counting time,  $t$  (min), as

$$\epsilon_I = \sqrt{\frac{d^2 R}{tY^2}} \quad (38)$$

where  $d$  = the appropriate number of standard deviations for the required probability level, and

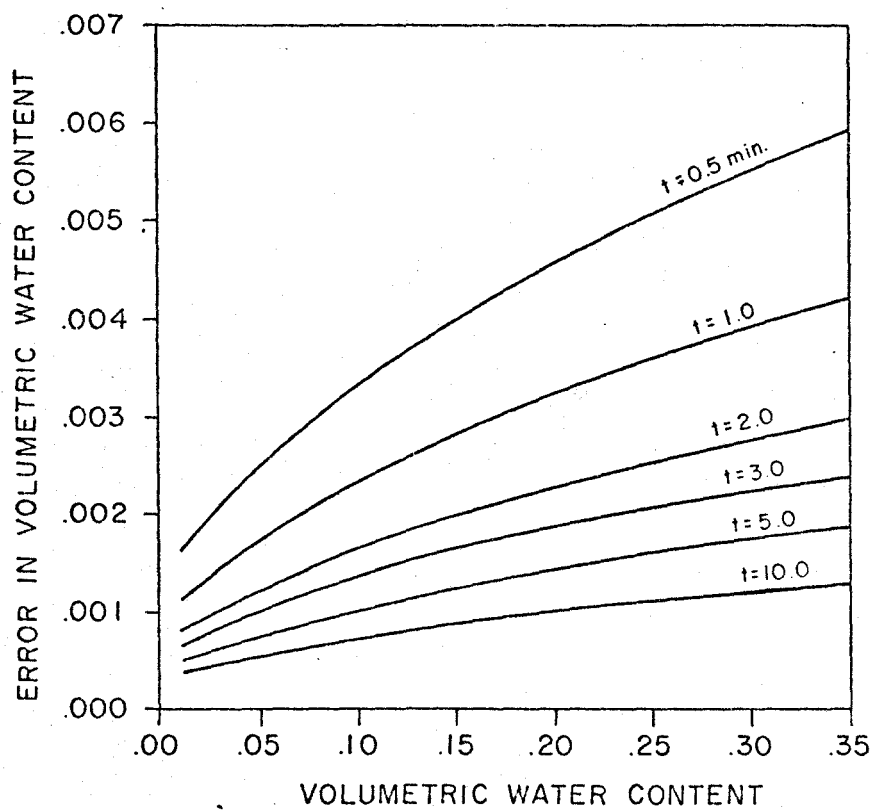
$Y$  = the sensitivity of the instrument, defined as the slope of the calibration curve (cpm/moisture volume fraction).

To give an indication of this error, eq. (38) has been solved for various counting times and moisture contents, using a probability level of 95 percent and a sensitivity of 80,452. The latter value was determined from the calibration of the equipment used in this study. Fig. 4 shows the results which indicate the benefit to be gained from a long counting time. However, this must be balanced against the opposing consideration of time available for field measurements. Hewlett et al. (1964) considered that increased spatial sampling was more important than longer counting times. There is no consensus of opinion on this matter but most investigators have used counting times between 0.5 and 2.0 minutes.

Six sampling sites were used in the present study (Fig. 3). Three of these (sites 2, 3, and 6) were located in the corn rows and three (1, 4, and 5) were between rows. The measurement program was divided into two separate time sequences. The first involved measurements at all six sites on a basic 4-day interval, using a 1-minute counting time for each neutron reading. The second involved daily measurements at site 5, using a 5-minute counting time.

A Nuclear Chicago 5810 neutron depth probe, with a Nuclear Chicago 5920 scaler, was used to measure moisture contents in 10 cm increments from 30 to 180 cm depth.

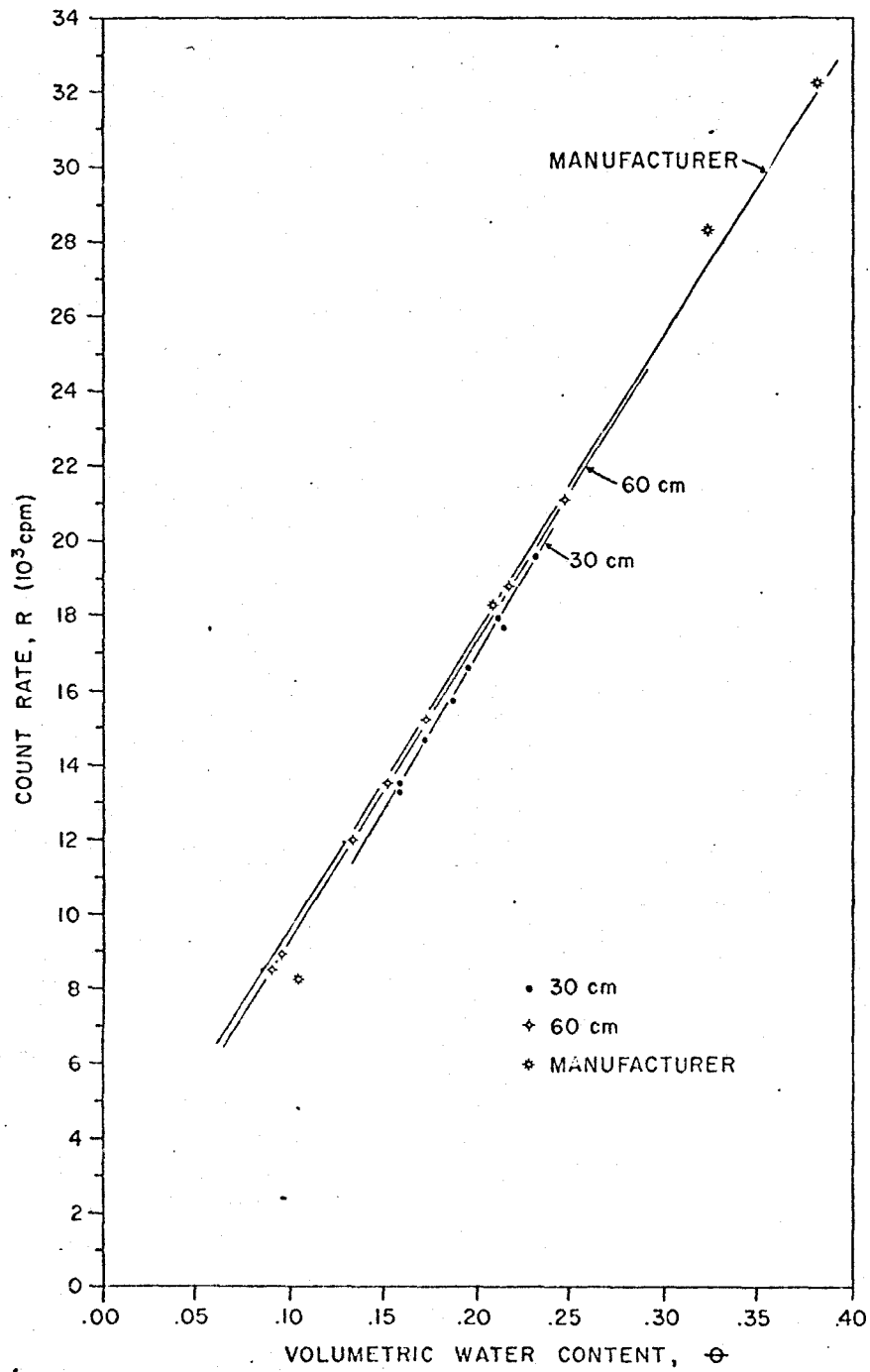
FIGURE 4  
COUNTING TIME ERRORS AT THE 95% PROBABILITY  
LEVEL



Thin-wall aluminum access tubes were installed to a depth of 220 cm. The installation procedure involved the removal of a soil core with a steel access tube of the same dimensions, and then inserting the aluminum tube. A rubber stopper was cemented into the bottom of the tube and a removable cork was placed on the top to prevent water accumulation. All readings were corrected for background count (which averaged about 225 cpm) and for coincidence loss. The latter was calculated using a response time of  $3.33 \times 10^{-7}$  min as suggested by the manufacturer, thus producing a correction of 30 cpm for an uncorrected count rate of 10,000 cpm.

The equipment was calibrated in the field at 30 and 60 cm depths to include both the sandy loam and the coarse sand. A 10-minute counting time for each calibration point ensured a minimal counting error. Volumetric moisture was determined from ten gravimetric samples, each 15 cm long, which were removed from around the access tube with a core sampler at a radius of 15 cm. Eighteen calibration points were obtained but three of these, obtained shortly after a heavy rainfall, were discarded because there were large vertical gradients in moisture content. The final calibration is shown in Fig. 5 and the regression constants for the calculated calibration

FIGURE 5  
NEUTRON DEPTH PROBE CALIBRATION



lines are presented in Table 1. There was good agreement between the field calibration and the manufacturer's calibration. The calibration obtained from the 30 cm depth was slightly different than that for 60 cm. At the same moisture content the count rate was lower at 30 cm than at 60 cm, probably the result of chemical differences in the soil since the mean densities at the two depths were almost identical ( $1.56$  and  $1.58 \text{ g cm}^{-3}$  at 30 and 60 cm, respectively) and the radius of the probe's volume of influence, calculated from the manufacturer's specifications, should not have exceeded 30 cm at moisture contents greater than 0.14. The calibration obtained at 30 cm was applied to the readings taken at 40 cm and above, and the 60 cm calibration was applied to all readings below 40 cm.

Table 1

Regression and correlation constants for neutron probe calibrations of the form  $\theta$  (volume fraction) =  $a + bR$  (cpm)

<u>Probe</u>	<u>a</u>	<u>b</u>	<u>Correlation coefficient</u>	<u>Standard error</u>
Depth				
30 cm	-0.0004	$1.18 \times 10^{-5}$	0.99	0.0024
60 cm	-0.0161	$1.24 \times 10^{-5}$	0.99	0.0008
Surface	0.0388	$1.26 \times 10^{-4}$	0.95	0.0108

Usually the neutron depth probe cannot be used within the top 20 or 30 cm of soil because fast neutrons escape into the air, thus nullifying the instrument's calibration. Several attempts have been made to extend the use of the depth probe to the surface layer (Pierpoint, 1966; Black and Mitchell, 1968; Luebs et al., 1968) but these have had limited success. A neutron surface probe can be used on a smooth flat soil surface but it is unsuitable for use where there is a dense plant growth.

Surface moisture contents can also be determined by the gravimetric method. This technique involves removing surface soil samples and drying them in an oven at 105°C for about 24 hours. The change in weight represents the amount of water originally held by the soil. The volumetric moisture content,  $\theta$ , is calculated as

$$\theta = \frac{W_w}{W_D} \times \rho_s \quad (39)$$

where  $W_w$  = the weight of water in the wet soil sample (g),  
 $W_D$  = the weight of dry soil (g),  
 $\rho_s$  = the bulk density of the dry soil ( $\text{g cm}^{-3}$ ), and  
 $W_w/W_D$  = the moisture by dry weight.

In this study the moisture content of the 25 cm surface layer was determined gravimetrically from ten soil samples taken at each site with a core sampler. It was

expected that the calculation of volumetric moisture could be performed using the individual bulk densities measured at a given site on a given date. However, this procedure produced erratic moisture changes because sample densities changed from measurement to measurement. Consequently the mean density of all the samples taken at a given site was used to calculate the volumetric moisture. These values are summarized in Table 2.

Table 2  
Soil densities ( $\text{g cm}^{-3}$ ) at each site

<u>Site</u>	<u>Mean density</u>	<u>Standard deviation</u>	<u>Number of samples</u>
1	1.28	0.15	80
2	1.49	0.13	80
3	1.29	0.23	80
4	1.47	0.11	80
5	1.38	0.16	400
6	1.22	0.20	80

Some measurements with a neutron surface probe (Nuclear Chicago 5901) were also made on the daily routine. Five 2-minute readings were taken each day, always on the same spots. Following the procedure of Bowman and King (1965) the moisture contents derived from these readings

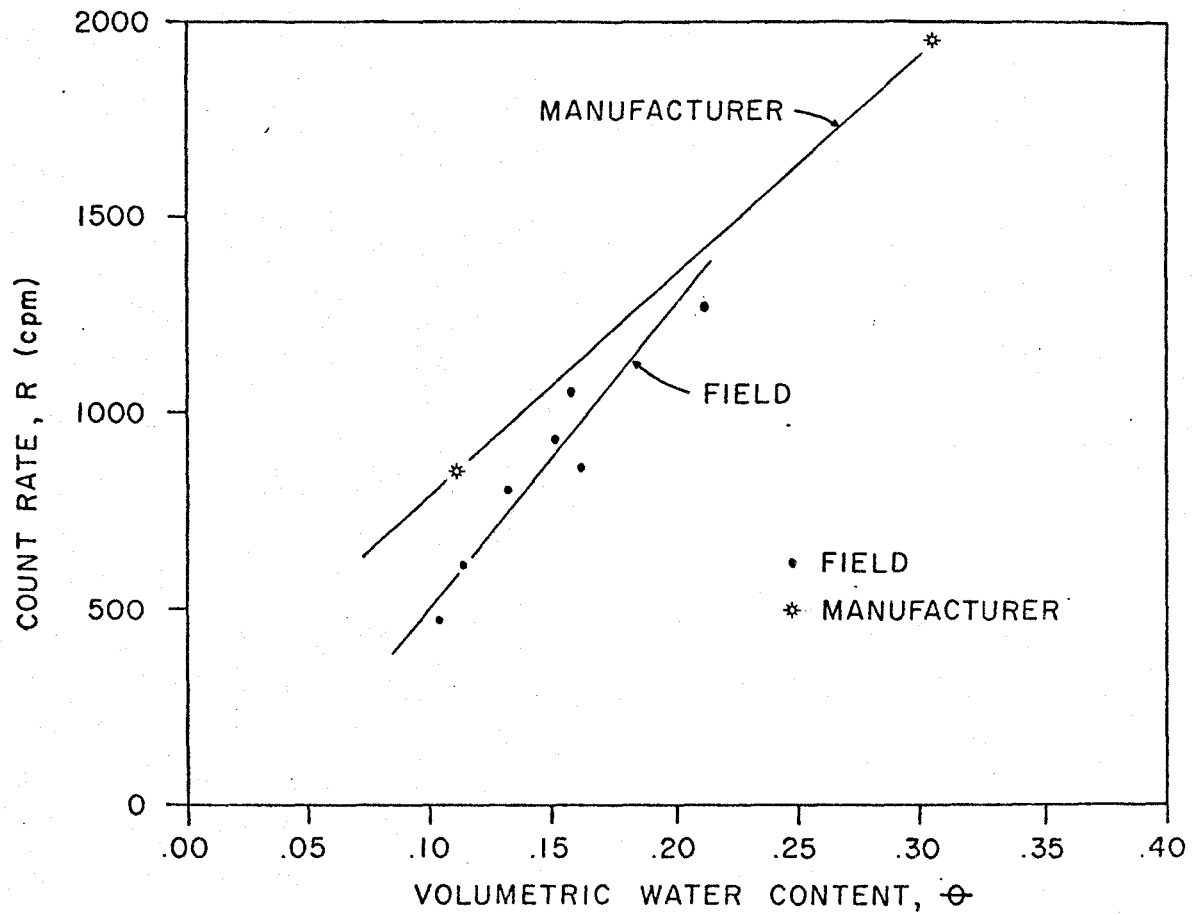
were considered representative of the top 15 cm layer of soil. An additional depth probe reading at the 20 cm depth represented the layer between 15 and 25 cm.

The calibration of the surface probe is shown in Fig. 6. A field calibration was performed by taking the average count rate from a total 20-minute count, the probe being turned through  $180^{\circ}$  after the first 10 minutes. The moisture content of the soil was determined from twelve gravimetric samples, each 15 cm in depth, which were taken from the spot on which the probe had been placed. Regression and correlation constants for the calculated calibration line are presented in Table 1.

### (iii) Drainage

The water drainage out of the test plot can be calculated from a knowledge of the hydraulic gradient and the capillary conductivity, as indicated in eq. (4). In this study, hydraulic gradients were measured with a series of soil moisture tensiometers arranged in a vertical profile. The tensiometer consists of a water-filled porous cup connected by a continuous water column to a mercury manometer. The moist porous cup is permeable to water and solutes but not to air. Flow of water through the cup walls brings the cup water into hydraulic equilibrium with the soil water, so that changes in soil water conditions are reflected by

FIGURE 6  
NEUTRON SURFACE PROBE CALIBRATION

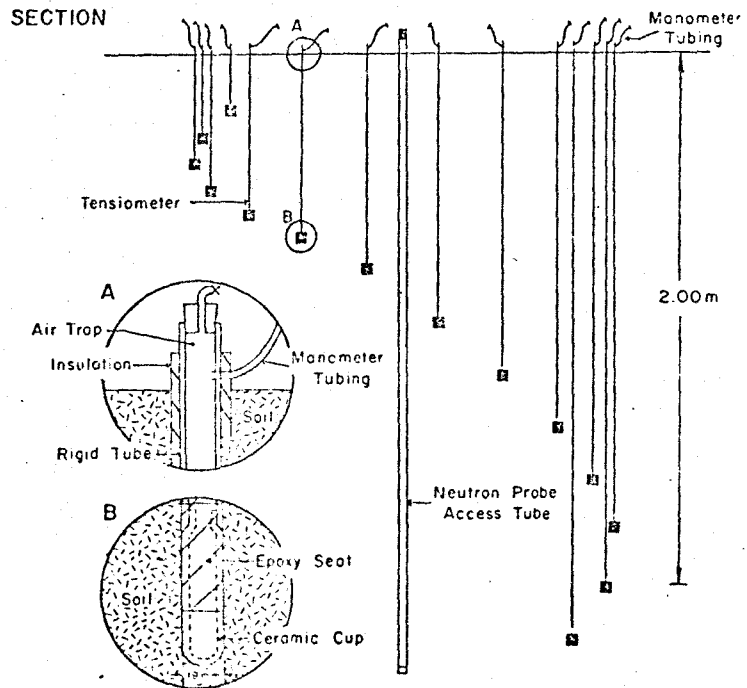
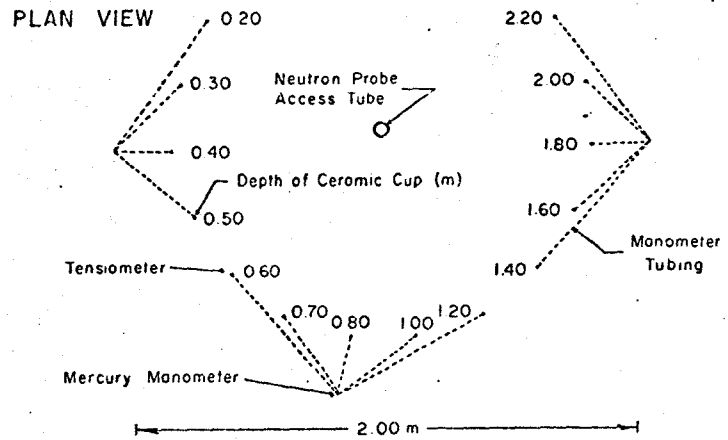


corresponding changes in the manometer reading. Since the manometer indicates partial vacuum relative to the atmosphere, the highest reading theoretically possible is 1020 cm of water. However, the practical limit is only about 800 cm because air enters the system at higher suction.

The instrumental design and arrangement were similar to those described by van Bavel et al. (1968b) and are illustrated in Fig. 7. All tensiometers were constructed using a porous ceramic cup with an outer diameter of 19 mm and 52 mm long. The open end of the cup was sealed by epoxy resin into a length of clear rigid plastic tubing of the same diameter. The sensing zone of each cup was reduced by sealing the top 27 mm with epoxy resin to define more precisely the depth to which the reading applied. The response time constant was 6 minutes as indicated in tests prescribed by Richards (1949).

Each tensiometer was tightly set into a vertical hole and was connected to a mercury manometer. The top part was insulated by pouring a jacket of styrofoam around the rigid tubing. All tensiometers were filled with deaerated (boiled distilled) water. When the manometer and connecting tubing had been purged, the manometer scale was adjusted to read hydraulic head (referenced to the soil surface) directly in cm of water. This is accomplished by

FIGURE 7  
ARRANGEMENT OF TENSIOMETERS



setting the scale zero at a distance,  $a$ , above the mercury surface in the vial such that

$$a = \frac{b\rho_w}{\rho_m - \rho_w} \quad (40)$$

where  $b$  = the vertical distance from the soil surface to the surface of the mercury in the vial (cm),

$\rho_w$  = the density of water ( $\text{g cm}^{-3}$ ), and

$\rho_m$  = the density of mercury ( $\text{g cm}^{-3}$ ).

Since  $\rho_w = 1.0 \text{ g cm}^{-3}$  and  $\rho_m = 13.5 \text{ g cm}^{-3}$ , eq. (40) reduces to

$$a = \frac{b}{12.5} \quad (41)$$

The tensiometers were refilled and purged with deaerated water whenever air bubbles appeared in the air trap.

Hydraulic head was measured at all six sites at four depths: 120, 140, 160, and 180 cm. Observations were made daily at 3-hour intervals between 0500 and 2000 hours EST. The terminal depth for the calculations of soil moisture change was chosen at 140 cm, so the hydraulic gradient at that depth was calculated as the average gradient between 120 and 160 cm. Profiles of hydraulic head at sites 1 and 5 were obtained from 20 to 220 cm. Between 20 and 80 cm depth the tensiometers were installed in 10 cm increments, and in 20 cm increments below 80 cm depth.

The readings of hydraulic head were affected by diurnal temperature changes, despite the insulation on the tensiometers. However, hydraulic gradients remained nearly constant throughout the day. Consequently, the gradients at 140 cm were computed from all of the readings, but moisture characteristics (the relationship between  $\psi$  and  $\theta$ ) have been prepared using only the readings taken at 0500 hours.

Both field and laboratory procedures are used to determine the relationship between  $k_z$  and  $\theta$  which is usually called the conductivity characteristic. A prerequisite for laboratory determinations is that the measuring system must closely approximate field conditions. Several difficulties have been encountered in this respect (Holmes et al., 1967), so field methods such as those described by Rose et al. (1965), Rose and Krishnan (1967), and by van Bavel et al. (1968b), are to be preferred.

The field methods are based on the equation

$$k_z = \frac{P - \Delta S_m - E}{-(d\phi/dz)} \quad (42)$$

where it is assumed that there is no horizontal water movement. The calculated value of  $k_z$  would apply to the mean moisture content at depth  $Z$ . Rose et al. (1965) and Rose and Krishnan (1967) have suggested that  $k_z$  may be

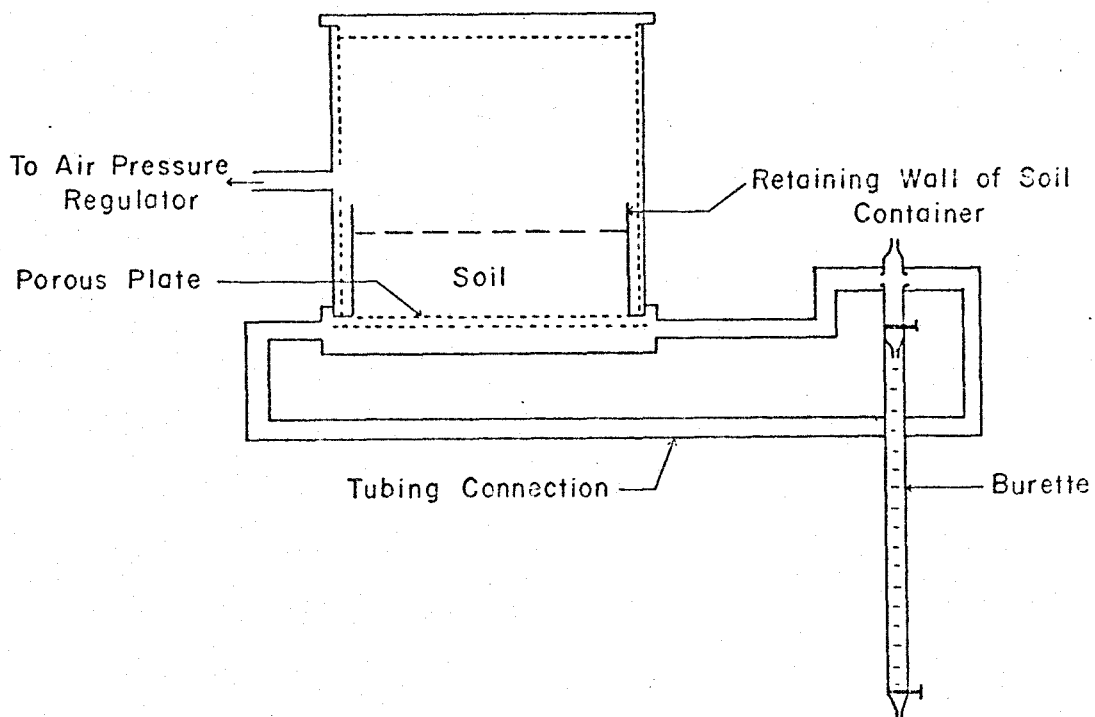
determined quite accurately by this method if P and E are eliminated from eq. (42) by covering the soil with a tarpaulin. This procedure was followed in the present study. After the crop had been harvested, the soil surface around each site was covered with sheets of plastic each measuring 4 x 4 m. Soil was piled on the edges of the plastic to keep it in contact with the ground.

The conductivity characteristic was also determined by the transient diffusion method as described by Gardner (1956). An undisturbed soil sample is placed in a pressure cell as shown schematically in Fig. 8. The soil is saturated with water and allowed to reach equilibrium at atmospheric pressure. When the cell is sealed and pressure is applied, water is forced from the soil through the porous ceramic plate and measured in a burette. This type of equipment has been used extensively to determine soil moisture characteristics but Gardner (1956) showed that the capillary conductivity could also be calculated if the rate of discharge was measured. The conductivity,  $k$ , is determined as

$$k = \frac{B O_o \rho_w g}{V \Delta P_I \alpha^2} \quad (43)$$

where  $B$  = the slope of the line obtained by plotting the natural logarithm of the outflow yet to be

FIGURE 8  
ILLUSTRATION OF PRESSURE CELL FOR MEASURING  
CAPILLARY CONDUCTIVITY OF SOIL



discharged ( $O_o - O$ ) against time,

$O_o$  = the total outflow from the sample for a given pressure increment ( $\text{cm}^3$ ),

$O$  = the outflow at any given time ( $\text{cm}^3$ ),

$\rho_w$  = the density of water ( $\text{g cm}^{-3}$ )

$g$  = gravitational acceleration ( $\text{cm sec}^{-2}$ ),

$V$  = the volume of the sample ( $\text{cm}^3$ ),

$\Delta P_I$  = the incremental pressure change (mbar), and

$\alpha$  = a constant for any sample ( $\text{cm}^{-1}$ ).

$\alpha$  is calculated as

$$\alpha = \frac{\pi}{2X} \quad (44)$$

where  $\pi = 3.14$ , and

$X$  = the length of the sample (cm).

The equation of the outflow curve is

$$\ln(O_o - O) = \ln \frac{8O_o}{\pi^2} - Bt \quad (45)$$

where  $t$  = the time between the pressure change and the observation of  $O$  (hours).

This equation may be used to determine the values of  $B$  for the solution of eq. (43).

Various other equations have been proposed to calculate conductivity values from a knowledge of the moisture characteristic. The common method is described by Marshall

(1958), whose equation was slightly modified by Millington and Quirk (1959, 1961). The procedure is to divide the moisture characteristic into a number of equal moisture classes, to determine the value of the matric suction which applies to the mid point of each class, and to calculate the conductivity from

$$k = M\theta^m n^{-2} \{ \psi_1^{-2} + 3\psi_2^{-2} + \dots + (2n-1)\psi_n^{-2} \} \quad (46)$$

where  $M$  = a constant which converts the effective pore radius to the matric suction in cm of water and converts the units into those for conductivity (see Marshall, 1958),

$\theta$  = the highest volumetric moisture content in the moisture class,

$\psi_n$  = the matric suction at the mid point in the  $n^{\text{th}}$  class (cm of water),

$m$  = 2 in the Marshall equation; 1.33 in the Millington and Quirk equation, and

$n$  = the number of moisture classes up to the water content of interest in the Marshall equation; the total number of classes in the Millington and Quirk equation.

Comparisons of measured and calculated values of conductivity have indicated that the Millington and Quirk equation produces reasonable conductivity characteristics if the

calculated values are multiplied by a matching factor (Jackson et al., 1965; Kunze et al., 1968). This matching factor is the ratio of the measured and calculated values at the same moisture content. Although the method is semi-empirical it does provide an easy way of checking conductivities determined by other procedures. Both the Marshall and the Millington and Quirk equations were used for that purpose in this study.

### 3. Measurements for the Energy Balance

Energy balance estimates of evapotranspiration were used as control data to test the water balance and equilibrium models. The necessary measurements included net radiation, soil heat flux, and temperature gradients and wet-bulb depressions above the crop.

#### (i) Net radiation

Net radiation was measured with a Funk-type net radiometer (Swissteco, Type S-1) which was positioned 1 m above the crop. Nitrogen was passed through the instrument to keep the polyethylene domes inflated, to equalise convective heat loss from each of the thermopile surfaces and to prevent internal condensation. The signal was continuously recorded on a Honeywell Electronik 194 2-pen strip chart recorder, and was subsequently integrated with a planimeter to give hourly totals of the flux. The

latter were calculated using a calibration of 115.8 mV/cal cm<sup>-2</sup> min<sup>-1</sup>, as determined by the National Radiation Laboratory, Meteorological Branch, Canada Department of Transport.

(ii) Soil heat flux

The soil heat flux,  $G$ , represents changes in energy storage in the ground, and theoretically this flux must be determined at the soil surface. However, a soil heat flux plate possesses considerably different radiative, thermal, and water-conducting properties from the soil around it. Consequently, it has been common practice to install the plate at a very shallow depth in the soil and to ignore any flux divergence which might occur between the soil surface and the plate. A much better procedure, described by Fuchs and Tanner (1968), is to install the plate at a slightly greater depth (5 to 10 cm) and to account for the divergence above it. In this case the flux,  $G$ , at the soil surface is given by

$$G = G_z + C \frac{\Delta \bar{T}_s}{\Delta t} \Delta Z \quad (47)$$

where  $G_z$  = the soil heat flux measured at depth  $Z$  (cal cm<sup>-2</sup> min<sup>-1</sup>),

- $C$  = the heat capacity of the soil between the surface and depth  $Z$  ( $\text{cal cm}^{-3} \text{ deg}^{-1}$ ),
- $\bar{T}_s$  = the mean soil temperature between the surface and depth  $Z$  ( $^{\circ}\text{C}$ ), and
- $t$  = time (min).

$C$  can be determined using a procedure described by van Wijk (1965). Since soil is composed of mineral and organic solid material, water, and air, its overall heat capacity can be calculated as

$$C = C_m X_m + C_o X_o + C_w \theta + C_a X_a \quad (48)$$

- where  $C_m$  = the heat capacity of the mineral matter ( $\text{cal cm}^{-3} \text{ deg}^{-1}$ ),
- $C_o$  = the heat capacity of the organic matter ( $\text{cal cm}^{-3} \text{ deg}^{-1}$ ),
- $C_w$  = the heat capacity of water ( $\text{cal cm}^{-3} \text{ deg}^{-1}$ ),
- $C_a$  = the heat capacity of air ( $\text{cal cm}^{-3} \text{ deg}^{-1}$ ),
- $X_m$  = the volume fraction of mineral matter,
- $X_o$  = the volume fraction of organic matter, and
- $X_a$  = the volume fraction of air.

$C_a$  is so small compared to the other heat capacities that it is safely neglected, and since  $C_w = 1.0 \text{ cal cm}^{-3} \text{ }^{\circ}\text{C}^{-1}$ , eq. (48) reduces to

$$C = C_m X_m + C_o X_o + \theta \quad (49)$$

Average values of  $C_m$  and  $C_o$  reported by van Wijk were 0.46 and  $0.60 \text{ cal cm}^{-3} \text{ }^\circ\text{C}^{-1}$ , so that

$$C = 0.46 X_m + 0.60 X_o + \theta \quad . \quad (50)$$

In this study,  $G$  was calculated as the sum of the flux at 5 cm and the divergence between 5 cm and the surface. The flux at 5 cm depth was measured with three transducers (Middleton and Pty. Ltd.) connected in series which had a combined calibration of  $43.79 \text{ mV/cal cm}^{-2} \text{ min}^{-1}$  as determined by the manufacturer. The signal was continuously recorded on the Honeywell recorder, and was integrated with a planimeter to give hourly totals. Hourly changes of the mean temperature in the 0-5 cm layer were monitored with a 5-junction thermopile. Junctions were located at 0.5, 1.0, 2.5, 3.5 and 5.0 cm with the reference thermopile installed at a depth of 160 cm. The heat capacity of the soil was found from eq. (50). The volumetric contents of mineral and organic matter were determined to be 0.459 and 0.024 respectively from "loss-on-ignition" treatments of five samples. This reduced eq. (50) to

$$C = 0.225 + \theta \quad . \quad (51)$$

The moisture content of the 0-5 cm layer was determined gravimetrically from ten samples taken at mid-morning at the soil heat flux site, and it was assumed that the value

remained constant throughout the day. A mean density of  $1.25 \text{ g cm}^{-3}$ , determined from 300 samples, was used for the volumetric calculations.

On July 12 one junction of the thermopile used to measure the soil temperature was broken and this was not noticed until July 17. Analysis of the existing data indicated that daily values ( $\text{cal cm}^{-2} \text{ day}^{-1}$ ) for the period 0500-2000 hours could be accurately predicted from the equation:

$$G = 0.0645 R_n + 1.0993 G_5 - 7.85 \quad . \quad (52)$$

The multiple correlation coefficient was 0.94 and the standard error was only  $6.18 \text{ cal cm}^{-2} \text{ day}^{-1}$ . Consequently, daily values of surface soil heat flux for the period July 12 - 17 were estimated from eq. (52).

(iii) Temperature gradients and wet-bulb depressions

The temperature and humidity mast is shown in Plate 1 and the components of the system are illustrated in Fig. 9. All temperature measurements were made with 5-junction thermopiles, similar to those described by Lourence and Pruitt (1969). They were made from standard 36 gage copper-constantan thermocouple wire, the junctions being enclosed in an aluminum sleeve. A stainless steel shaft, attached to the aluminum sleeve, served to encase the wires and provide rigidity. Two thermopile units were

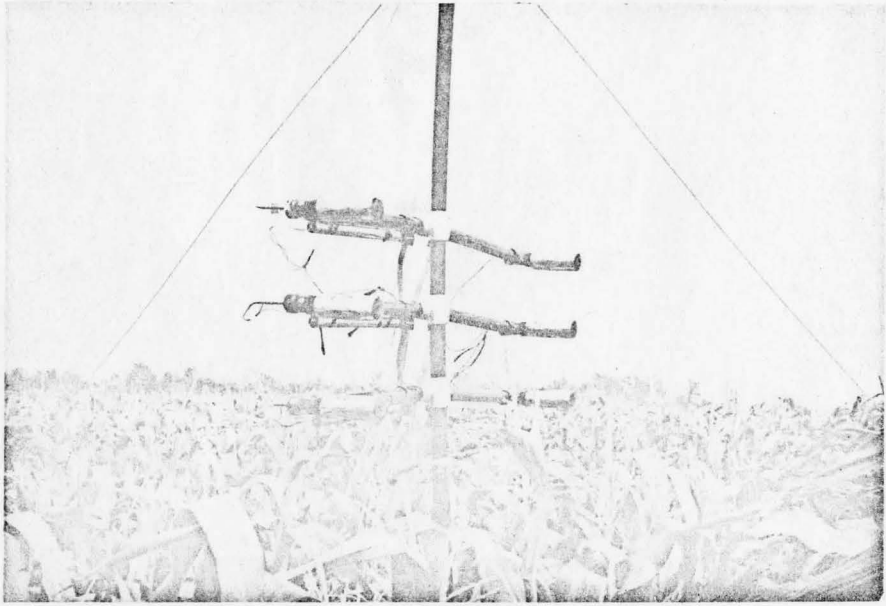
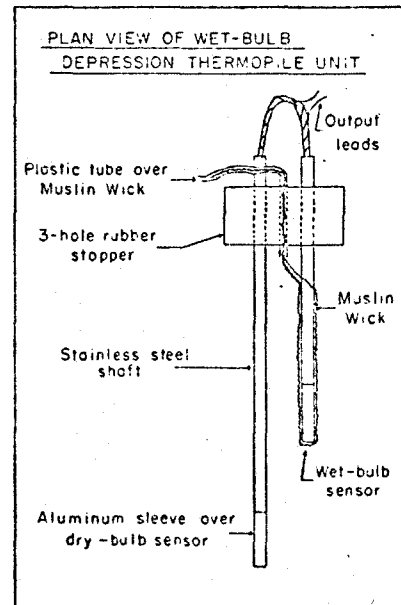
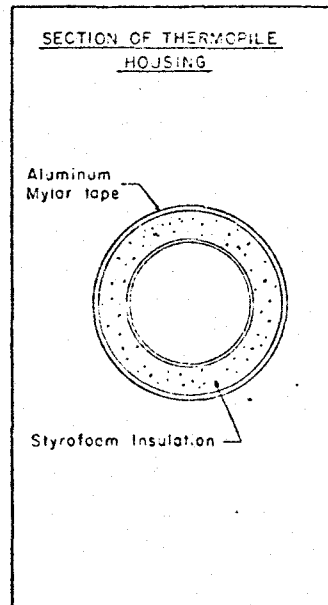
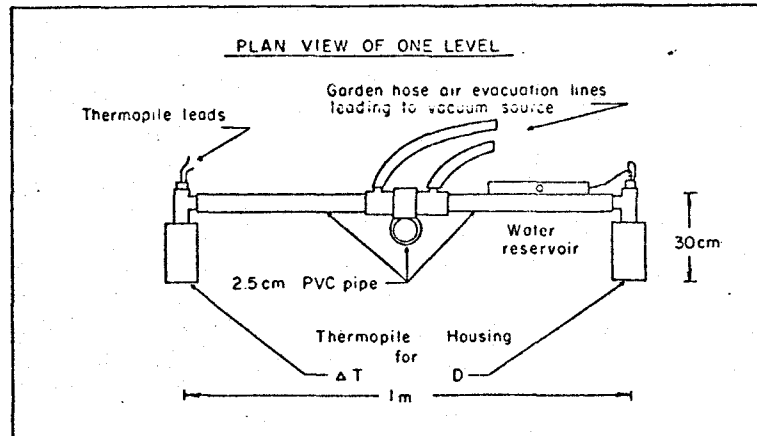


Plate 1

Temperature and humidity mast.

FIGURE 9  
ILLUSTRATION OF TEMPERATURE AND HUMIDITY  
MEASUREMENT SYSTEM



individually calibrated against platinum resistance temperature sensor standards and were found to have an output of  $203 \text{ uV } ^\circ\text{C}^{-1}$ . The equation of the calibration line for the two units was

$$\Delta T = 0.0090 + (4.913 \times \text{OUTPUT (mV)}) \quad (53)$$

which had a standard error of  $0.007 \text{ }^\circ\text{C}$ . This calibration was assumed to be valid for all of the units.

The mast consisted of a 3-level system which was provided with two radiation shields on each level. One shield at each level contained a pair of thermopiles to measure wet-bulb depression directly. The other shield was used to measure directly the dry-bulb temperature difference between levels. An additional dry-bulb thermopile was included at the middle level to provide a measure of the absolute dry-bulb temperature. The companion unit was located at a depth of 130 cm in the soil to provide a stable temperature reference, the temperature of which was monitored with another unit referenced to ice water. The sensors in the radiation shields were aspirated from a common vacuum source which provided an aspiration rate of between  $4.5$  and  $4.8 \text{ m sec}^{-1}$  in the housings.

There is little agreement in the literature on the minimum height : fetch ratio required to ensure boundary layer conditions. Rule-of-thumb estimates range from 1:20

(Priestley, 1959) to 1:200 (Dyer, 1963), but most investigators have adopted intermediate values between 1:50 and 1:100. These latter values were suggested by Lettau (1959) and Slatyer and McIlroy (1961), respectively. Since a standard rule is not applicable to all situations, Penman et al. (1967) suggested that height : fetch relationships need to be determined for individual sites. Davies and McCaughey (1968) carried out investigations in a field adjacent to the one used in the present study, and found that boundary layer conditions were fulfilled for a ratio of 1:93. In this study, the three measurement levels were maintained at heights of 10, 35, and 60 cm above the crop, and minimum and maximum fetches were 41 m (E) and 128 m (SW), respectively. The top level had height : fetch ratios from 1:68 to 1:213, while the corresponding values for the middle level were 1:117 and 1:366. These ratios would appear to satisfy most requirements. Measurements at the top level were disregarded during easterly winds because of the relatively small fetch.

All temperature signals were recorded on a Solatron data acquisition system (Compact Logger Series 1) with a resolution of 2.5  $\mu\text{V}$ , which gives a 0.01  $^{\circ}\text{C}$  sensitivity to  $\Delta T$  and D measurements. Data were extracted from the teleprinter record for every second minute from 0500 to 2000 hours EST. Hourly values of the Bowen Ratio and

evapotranspiration were computed by a CDC 6400 computer for each of three air layers: 10 - 35 cm, 35 - 60 cm, and 10 - 60 cm. The three evapotranspiration values usually differed by less than  $0.03 \text{ cal cm}^{-2} \text{ min}^{-1}$ . Occasional instrumental failures, such as an insufficient water feed to one of the wet-bulb sensors, interrupted the evapotranspiration records for the two air layers affected by that measurement.

Daily evapotranspiration values were calculated as the sum of the hourly values for the layer in which records were consistently valid. A continuous record of evapotranspiration was obtained for the period July 1 - 25, with the exception of two hours on July 4 when the teleprinter was out of order.

#### 4. Calculations for the Equilibrium Model

Equilibrium evapotranspiration was calculated from the energy balance data. The value of S was determined from the mean hourly air temperature at the 60 cm height. Hourly equilibrium values were computed in the same computer program which performed the energy balance calculations, and were then summed to give daily totals.

## CHAPTER 4

### ENERGY BALANCE COMPONENTS AND EVAPOTRANSPIRATION

#### ESTIMATES FROM THE WATER BALANCE MODEL

##### 1. Energy Balance Regime

Daily variations of the energy balance components during the study period are shown in Fig. 10. Fair weather was experienced during most of the period and the majority of daily net radiation totals exceeded  $300 \text{ cal cm}^{-2} \text{ day}^{-1}$ . An average of 72 percent of the net heat available was utilized by the evapotranspiration process.

Bowen Ratio values shown in Fig. 11, had a mean of  $\beta = 0.34$  and ranged from a maximum of  $\beta = 0.99$  on July 8 to a minimum of  $\beta = -0.11$  on July 18. The ratio was high on three consecutive days (July 6 - 8) when the net radiation values were high and the canopy of the crop was not completely shading the soil surface. Small negative values of  $\beta$  occurred on two days, July 10 and July 18, indicating that there was a net transfer of sensible heat to the surface rather than away from it. As seen in Fig. 14, rains occurred on both of these days. Negative values of the sensible heat flux also occurred on other rainy days but they persisted for shorter periods of time so that the net daily transfer of sensible heat was positive.

FIGURE 10  
 VARIATION OF ENERGY BALANCE COMPONENTS  
 DURING JULY 1969

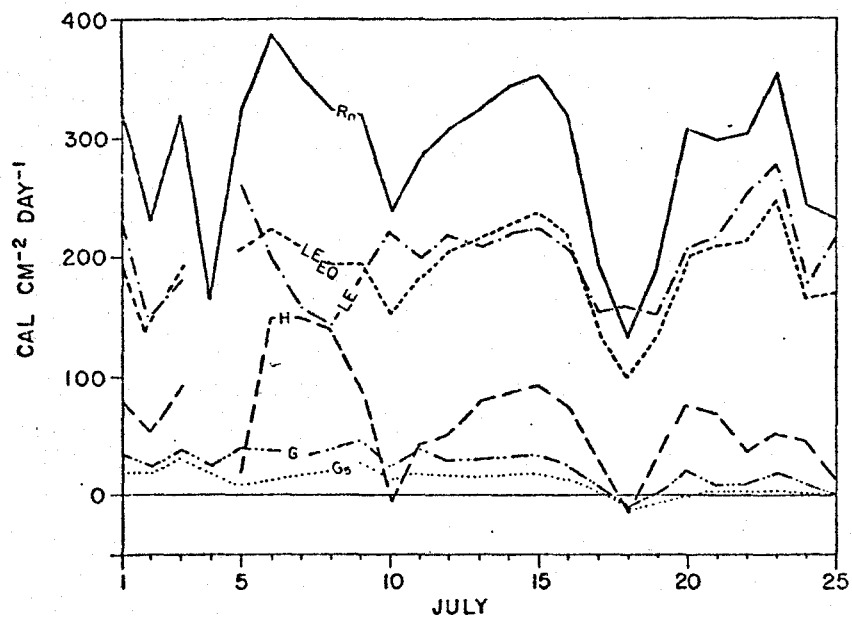
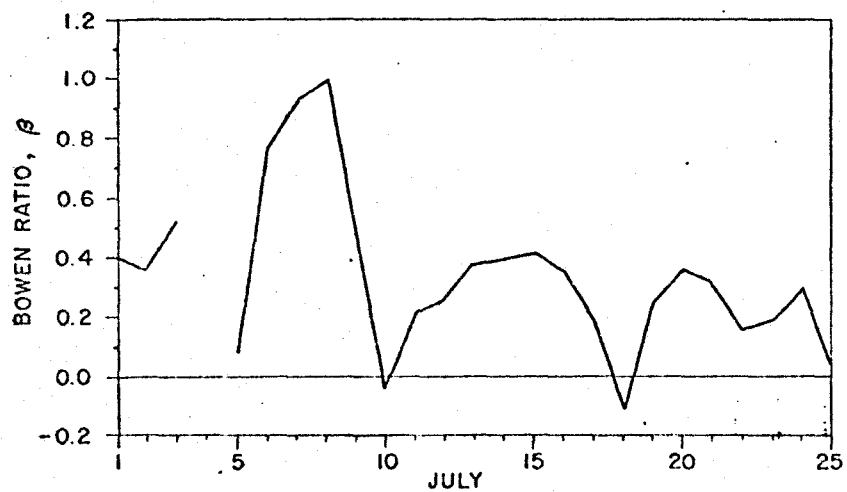


FIGURE 11  
 VARIATION OF DAILY BOWEN RATIO VALUES  
 DURING JULY 1969



The soil heat flux divergence between the flux plate and the soil surface was found to be a very important component of the total flux at the surface. Trends of the ratios  $G/R_n$  and  $G_5/R_n$  for daily values are shown in Fig. 12. The value at the surface always exceeded that at the 5 cm depth, and over the entire period the mean values of the ratios were 0.083 at the surface and 0.042 at the 5 cm depth. Measurements uncorrected for the divergence term would therefore have been in error by an average of nearly 100 percent. There was a general decrease in the values of both ratios, as well as in the magnitude of the divergence, as the crop continued to grow. This general decline indicates that the divergence may become insignificant on a daily basis for tall fully-developed crops, but is very important during crop development. This was particularly true in the present study because the plants were arranged in widely-spaced rows. It is even more important to account for the soil heat flux divergence when considering hourly, rather than daily, periods. Hourly values of the energy balance component fluxes on July 6 are shown in Fig. 13. The divergence was greatest in the morning and late afternoon hours, but was almost negligible during a 4-hour period in the early afternoon. Positive divergence values in the late afternoon were characteristic of sunny days at the beginning of July. This was the result of strong heating of the soil surface when

FIGURE 12

TRENDS OF THE RATIOS  $G/R_n$  AND  $G_5/R_n$  ON A DAILY BASIS  
DURING JULY 1969.

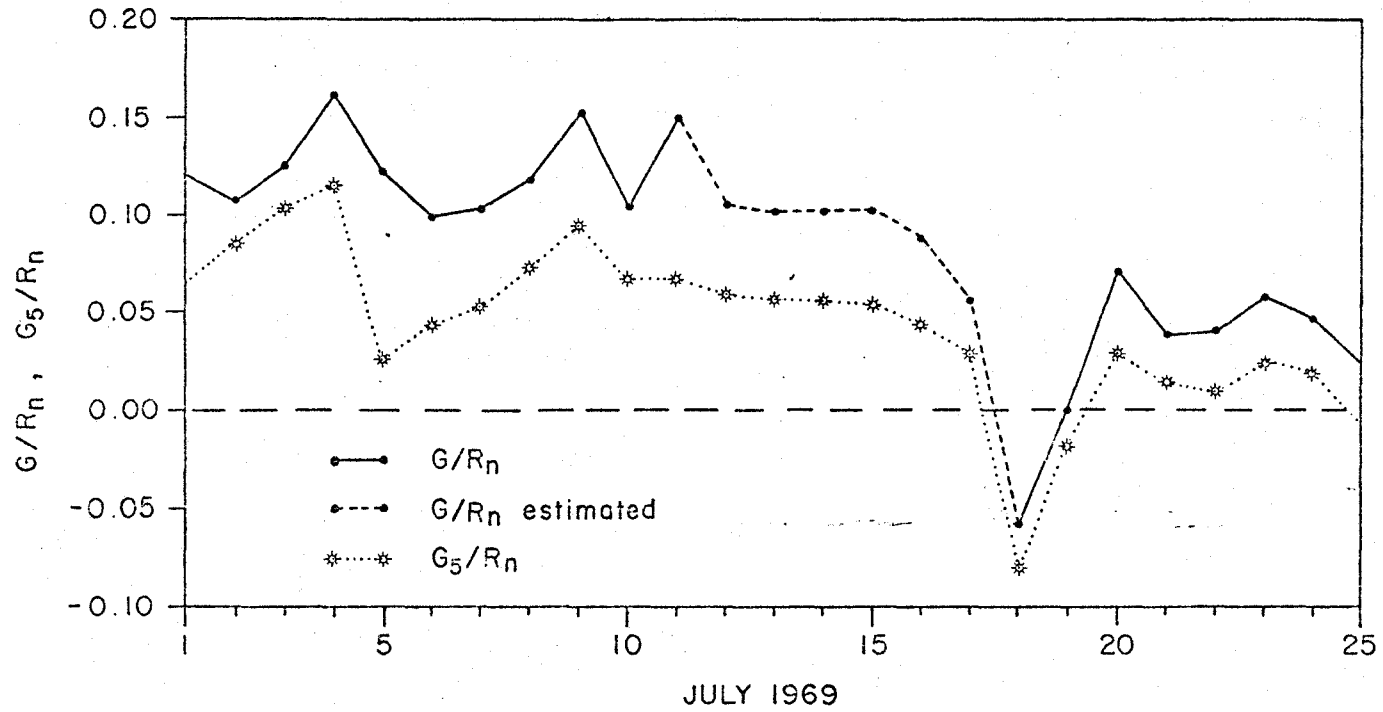
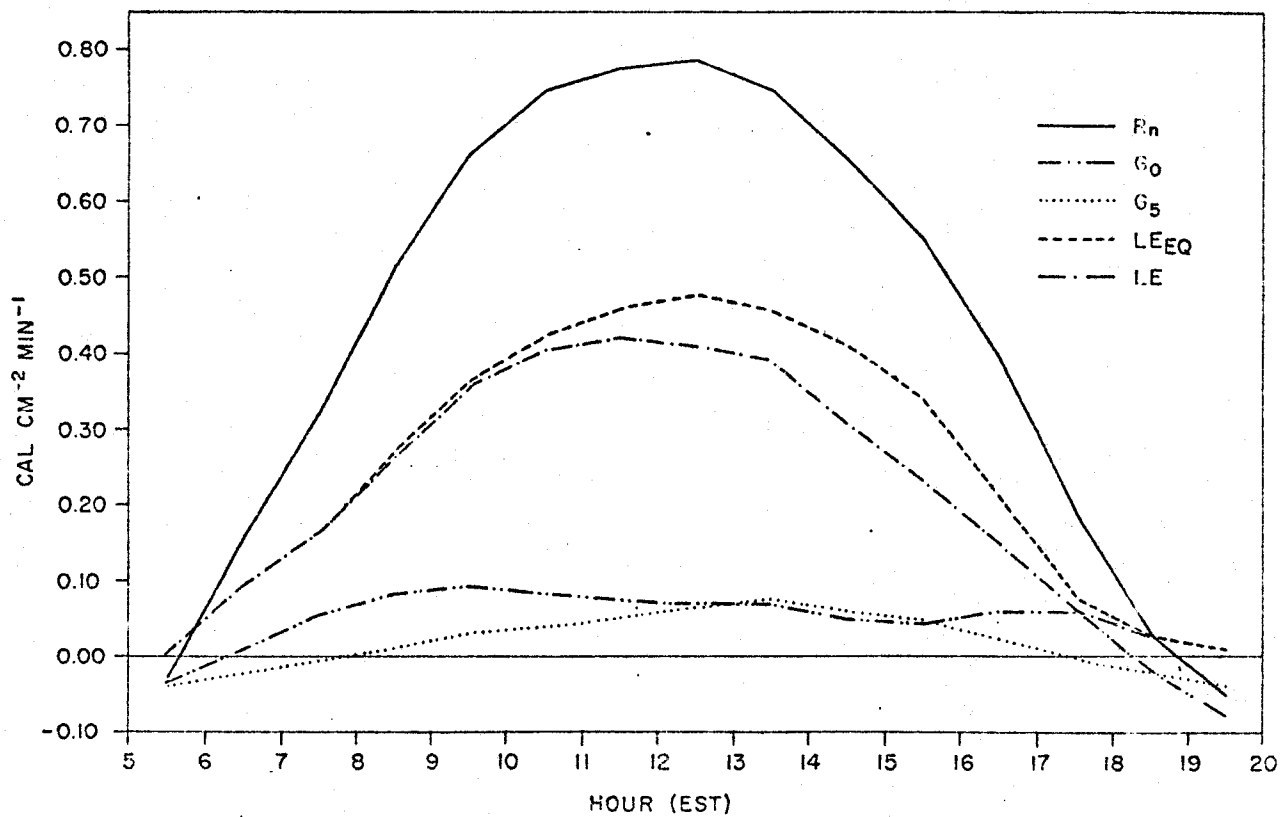


FIGURE 13  
VARIATION OF ENERGY BALANCE COMPONENTS AND EQUILIBRIUM  
EVAPOTRANSPIRATION ON JULY 6, 1969



the sun shone down the corn rows. During the latter part of the month the divergence term was usually negative at that time of day, a feature which was caused by the development of the plant leaves until they shaded the soil between the rows.

## 2. Water Balance Regime

The variations of precipitation and soil moisture storage during the study period are shown in Fig. 14. There were six days on which the total rainfall was light or moderate, not exceeding 14 mm in a single day. On July 25 there was an intense thunderstorm which gave 34 mm in a half hour. There was an average of 165 mm of soil moisture in the 140 cm profile, which represents an average moisture content of nearly 12 percent by volume. The average decrease in soil moisture was 39 mm during the month. However, as shown in Fig. 14, there was a considerable variation in both the absolute amounts and the changes of soil moisture at the six sites.

Fig. 15 shows daily and 4-day values of  $(P - \Delta S_m)$  during the study period. These values represent the water balance estimates of evapotranspiration which have not been corrected for water drainage from the soil profile. The daily values are widely scattered and include both large positive values and some negative estimates. The 4-day

FIGURE 14

VARIATION OF PRECIPITATION AND SOIL MOISTURE STORAGE  
DURING JULY 1969

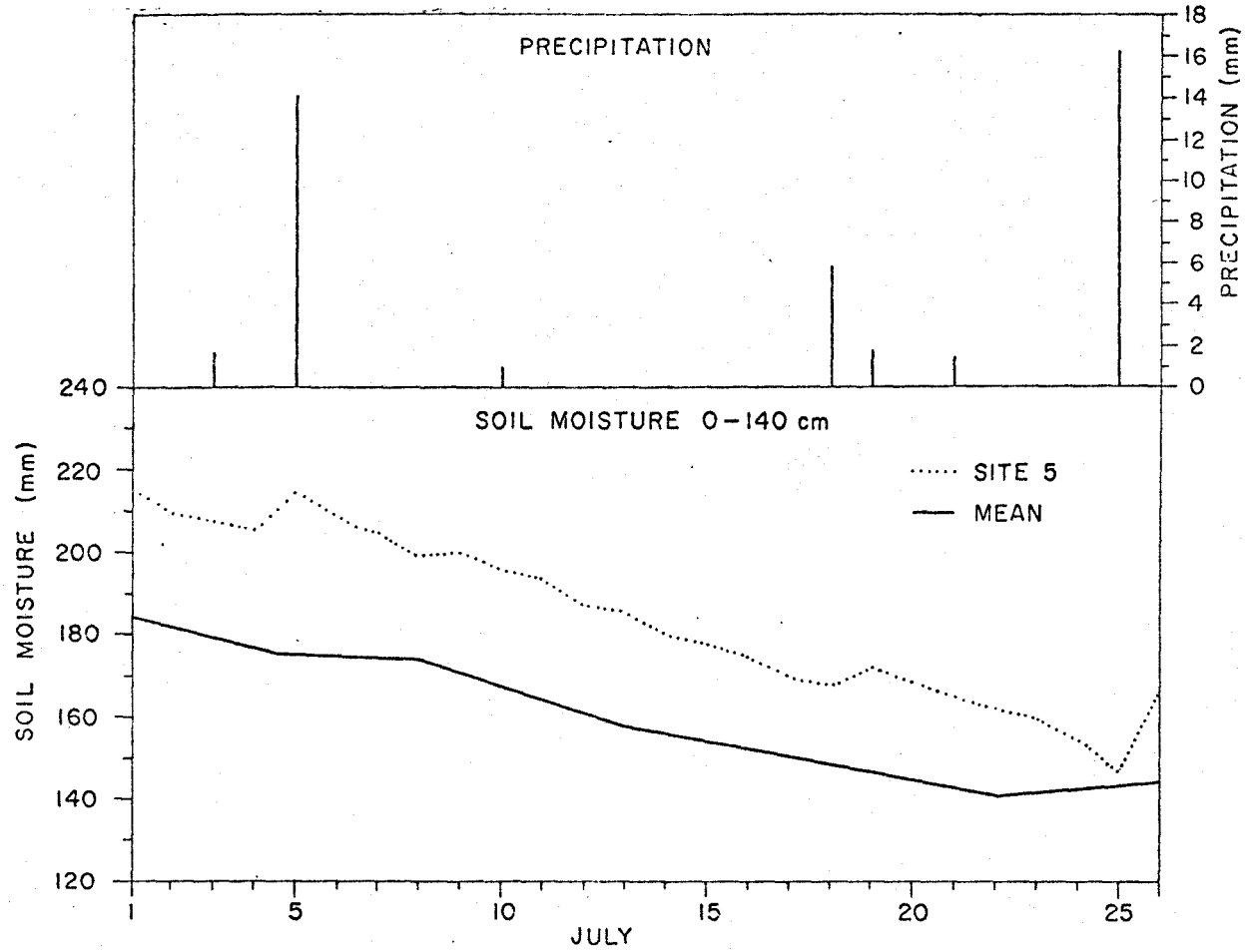
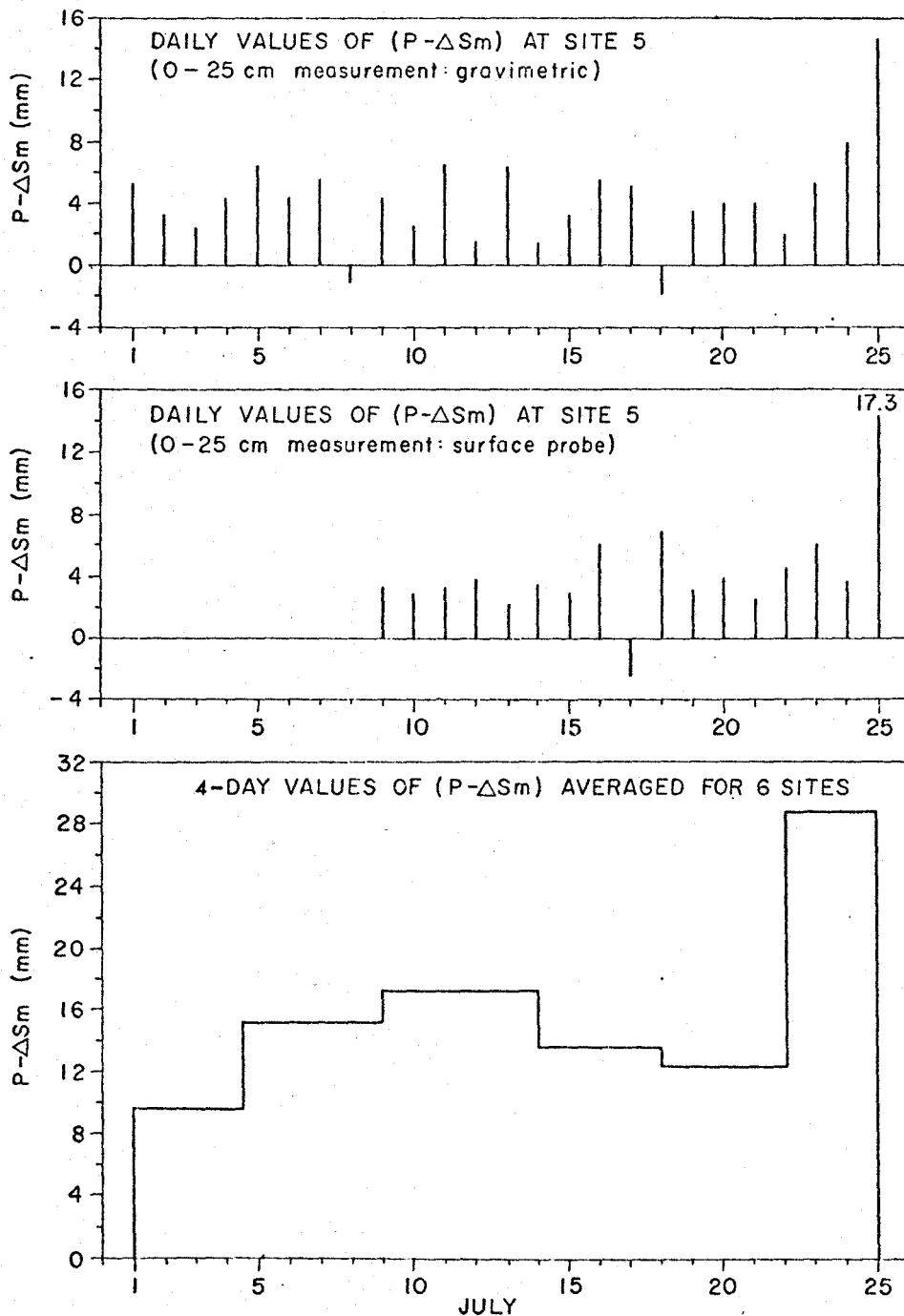


FIGURE 15  
 DAILY AND 4-DAY VALUES OF (P- $\Delta$ S<sub>m</sub>) DURING  
 JULY 1969



UNIVERSITY OF CALIFORNIA

values, averaged for the six sites, appear more reasonable with the exception of the value for the last period.

### 3. Evapotranspiration Estimates from the Water Balance

#### (i) Accuracy of the estimates

Daily values of  $(P - \Delta Sm)$  are plotted against the corresponding energy balance estimates of evapotranspiration in Figs. 16A and 16B. In the first case the surface soil moisture was measured gravimetrically and in the second with the neutron surface probe. Both methods produced a considerable scatter of points indicating that the resolution of the method was not sufficient to justify daily measurements.

In Fig. 17A the water and energy balance estimates for 4-day periods have been compared. The agreement between the two methods is very good except for one case. This anomalous point represents the period July 22 - 25 and includes the severe thunderstorm of July 25 which produced considerable surface runoff from the field. Since the runoff was not measured this loss of water led to an overestimation in the water balance calculations. The good agreement indicated in Fig. 17A may have been fortuitous. Values of soil moisture change in that diagram are means for six sites. When values of  $\Delta Sm$  from individual sites are used instead of the mean values (Fig. 17B) there is a considerable

FIGURE 16

RELATIONSHIPS BETWEEN DAILY VALUES OF E FROM THE ENERGY BALANCE AND  $(P - \Delta S_m)$  WHEN THE MOISTURE CONTENT OF THE 25CM SURFACE LAYER WAS MEASURED BY (A) THE GRAVIMETRIC METHOD AND (B) THE NEUTRON SURFACE PROBE

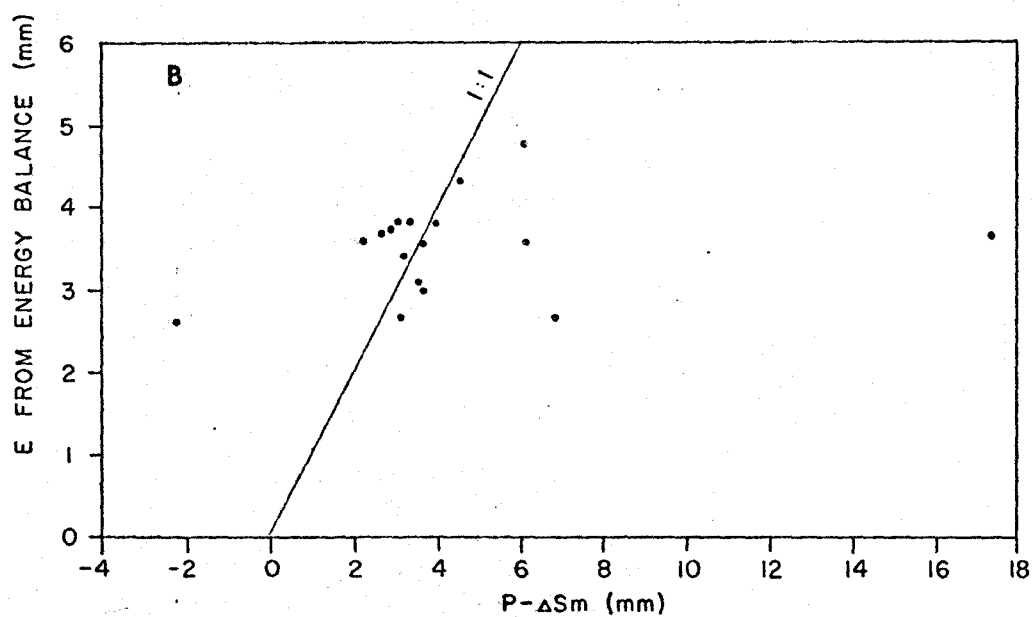
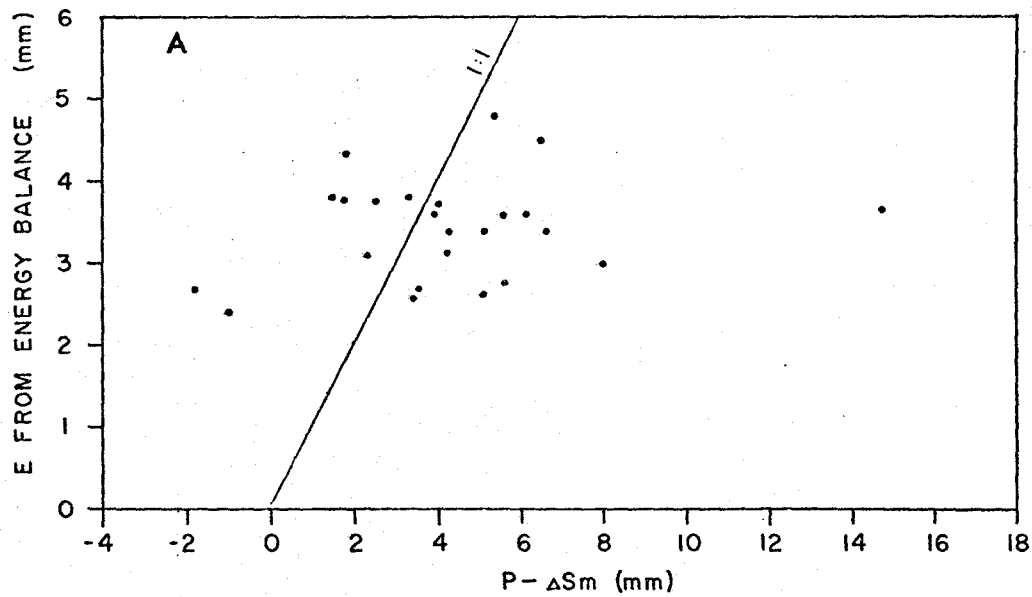
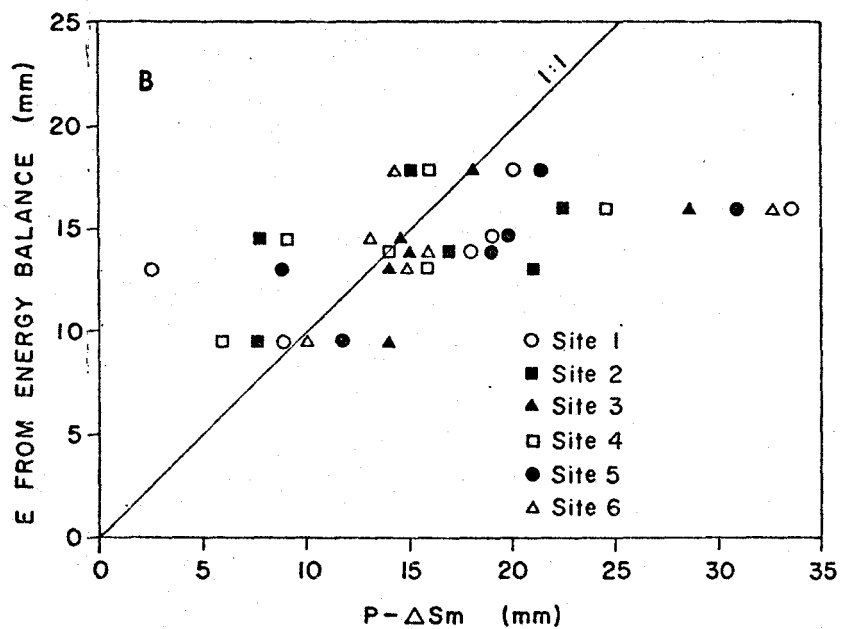
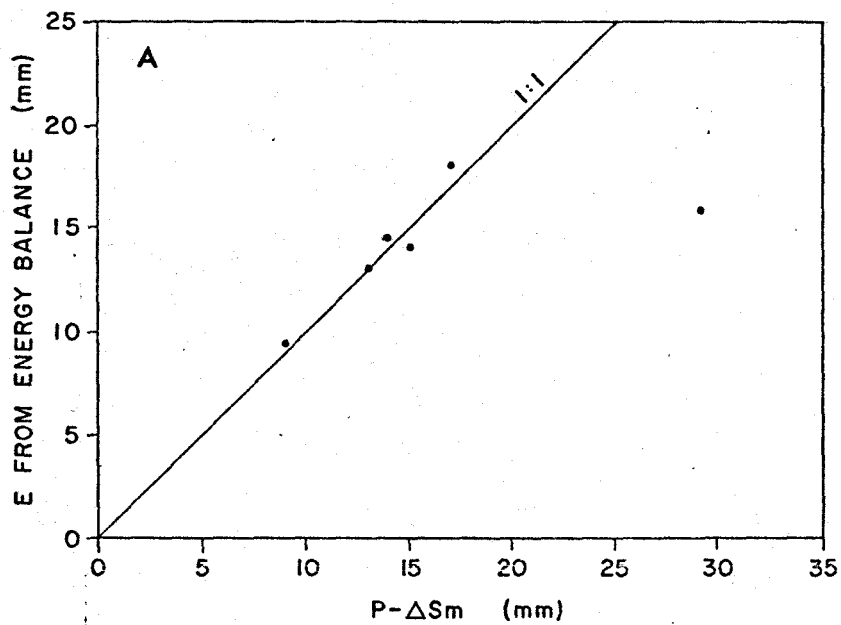


FIGURE 17

RELATIONSHIPS BETWEEN 4-DAY TOTALS OF E FROM THE ENERGY BALANCE AND (A) MEAN VALUES OF  $(P-\Delta S_m)$  AND (B) INDIVIDUAL VALUES OF  $(P-\Delta S_m)$



scatter due to large site-to-site variations.

(ii) Spatial variations in  $\Delta S_m$

A summary of the  $\Delta S_m$  values, together with precipitation, is presented in Table 3. Coefficients of variation (standard deviation/mean) ranged from 16 percent for July 9 - 13 to 93 percent for July 22 - 25. For the entire period from July 1 - 25, during which an average soil moisture loss of 43 mm was measured, there was a maximum difference of nearly 25 mm between sites. Such large differences were unexpected because of the close grouping of the six sites. Three factors may have accounted for the measured differences in  $\Delta S_m$ , and include locational differences, depth differences, and instrumental response changes.

Locational differences may have arisen because three access tubes were located in plant rows and the other three were between rows. One would expect that such differences in  $\Delta S_m$  values would be partially obscured because gravimetric samples for the surface layer were not restricted to "in row" and "between row" locations. This tends to be confirmed by the  $\Delta S_m$  values shown in Table 3. However, a correlation coefficient matrix for (P -  $\Delta S_m$ ) values, shown in Table 4, indicates some locational grouping. There was very good agreement between sites 1 and 5, both located between rows, and also between sites 3 and 6 which were located in rows.

Table 3

Precipitation (P) and soil moisture change ( $\Delta S_m$ ) in mm at  
six sites from July 1 to July 25

Period	P	$\Delta S_m$						Mean	Standard deviation
		Site 1	Site 2	Site 3	Site 4	Site 5	Site 6		
July 1 - 4	1.60	-7.24	-5.83	-12.18	-4.55	-9.52	-8.43	-7.96	2.73
4 - 8	13.26	-2.61	-1.96	-0.95	-0.14	-4.42	-1.81	-1.98	1.47
9 - 13	0.89	-18.97	-14.12	-16.77	-14.34	-19.70	-13.69	-16.27	2.62
14 - 17	5.05	-13.92	-2.12	-8.74	-3.94	-14.62	-7.71	-8.51	5.08
18 - 21	4.04	+1.96	-17.18	-10.00	-11.38	-4.59	-10.78	-8.66	6.57
22 - 25	33.78	+0.40	+11.64	+5.09	+9.09	+2.87	+0.57	+4.94	4.61
Total	58.62	-40.38	-29.57	-43.55	-25.26	-49.98	-41.85	-38.44	

There is no indication that this pattern applied to either site 2 (in row) or site 4 (between rows).

Table 4

Correlation coefficient matrix for (P -  $\Delta S_m$ ) values

Site	1	2	3	4	5
2	0.20				
3	0.83	0.60			
4	0.62	0.89	0.87		
5	0.99	0.29	0.85	0.69	
6	0.77	0.70	0.96	0.92	0.81

The influence of depth differences in the profile can be traced by calculating soil moisture change by layers. The 140 cm profile was divided into 3 layers: 0-25, 25-80, and 80-140 cm. This division arose from two considerations. Firstly, the 25 cm level separated an upper zone where soil moisture was determined gravimetrically from a lower zone where the neutron depth probe was used. Secondly, an examination of hydraulic head profiles at sites 1 and 5 (Fig. 18) showed that the 80 cm level separated regimes of upward and downward moisture movement. The calculated soil moisture changes in these layers are shown in Tables 5, 6, and 7.

FIGURE 18

PROFILES OF HYDRAULIC HEAD AT SITES 1 AND 5 ON SELECTED DAYS DURING JULY 1969

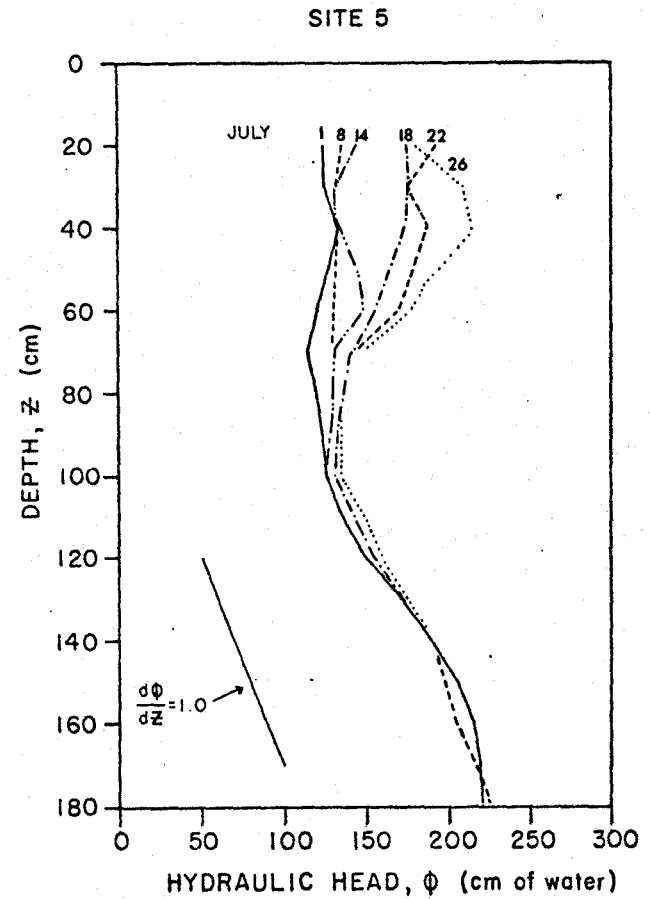
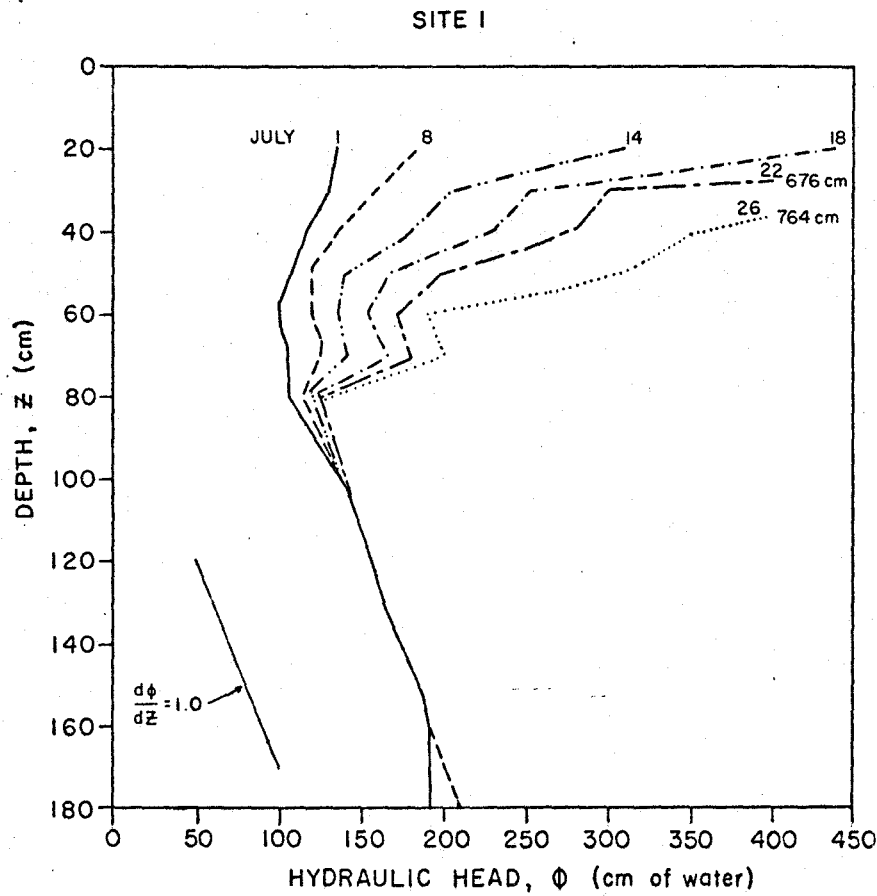


Table 5

Soil moisture change (mm) in the 0-25 cm layer

Period	Site 1	Site 2	Site 3	Site 4	Site 5	Site 6	Mean	Standard deviation
July 1 - 4	-2.65	0.58	-3.47	-0.59	-1.00	-1.98	-1.52	1.47
4 - 8	-4.64	-3.69	-2.12	-1.03	-3.96	-1.07	-2.75	1.56
9 - 13	-8.73	-5.07	-4.79	-5.42	-5.95	-3.14	-5.52	1.84
14 - 17	-7.10	4.78	4.50	1.77	-4.79	0.76	-0.01	4.90
18 - 21	5.53	-13.99	-3.57	-6.79	0.31	-7.77	-4.38	6.79
22 - 25	-0.03	11.96	9.45	8.74	8.85	5.03	7.33	4.24
Total	-17.62	-5.43	0.00	-3.32	-6.34	-8.17	-6.85	

Table 6

Soil moisture change (mm) in the 25-80 cm layer

Period	Site 1	Site 2	Site 3	Site 4	Site 5	Site 6	Mean	Standard deviation
July 1 - 4	-4.23	-4.27	-4.79	-1.75	-6.21	-5.16	-4.40	1.49
4 - 8	1.56	1.26	1.02	1.11	-0.31	-0.76	0.65	0.94
9 - 13	-8.47	-7.48	-8.29	-7.13	-9.77	-9.30	-8.41	1.02
14 - 17	-6.93	-6.07	-10.66	-4.02	-8.50	-8.18	-7.39	2.29
18 - 21	-2.39	-2.52	-4.62	-3.30	-3.17	-2.22	-3.03	0.89
22 - 25	0.63	-0.15	-2.32	0.99	-3.63	-3.97	-1.41	2.18
Total	-19.83	-19.23	-29.66	-14.10	-31.59	-29.59	-23.99	

Table 7

Soil moisture change (mm) in the 80-140 cm layer

Period	Site 1	Site 2	Site 3	Site 4	Site 5	Site 6	Mean	Standard deviation
July 1 - 4	-0.39	-2.15	-3.93	-2.21	-2.32	-1.29	-2.05	1.18
4 - 8	0.50	0.46	0.14	-0.22	-0.16	0.03	0.12	0.30
9 - 13	-1.78	-1.59	-3.69	-1.81	-3.98	-1.28	-2.35	1.17
14 - 17	0.12	-0.82	-2.57	-1.69	-1.34	-0.28	-1.10	0.98
18 - 21	-1.21	-0.68	-1.82	-1.32	-1.74	-0.80	-1.26	0.47
22 - 25	-0.18	-0.16	-2.07	-0.61	-2.44	-0.48	-0.99	1.00
	-2.94	-4.94	-13.94	-7.86	-11.98	-4.10	-7.63	

All layers contributed significantly to the variations in  $\Delta S_m$  for the entire profile, although the surface layer variations were usually greatest.

Possible change in instrumental response, would be indicated by the shield count for the neutron probe. A 1-minute shield count was obtained at each site to check the behaviour of the instrument. According to the manufacturer, a variation of  $\pm 3$  percent about the mean value is acceptable. Out of a total of 70 observations, only 3 exceeded this limit. Further, a plot of the change in shield count against the change in soil moisture content indicated no relationship between these two parameters.

(iii) Error analysis of  $\Delta S_m$  estimates

An analysis of measurement errors was performed in a final attempt to explain the variations in  $\Delta S_m$  values. The basic procedures were derived from analysis methods presented by Cook and Rabinowicz (1963) which were adapted to calculate the errors in the estimates of  $S_m$  and  $\Delta S_m$ . All errors are considered to be independent of one another and all calculations have been made for a 95 percent probability level.

The two possible errors in the gravimetric analysis include error in the determination of mean moisture by dry weight and error in determining the mean dry bulk density. The percentage error in the mean moisture by dry weight,  $\epsilon_{DW}$ ,

at the 95 percent confidence level is calculated as

$$\epsilon_{DW} = \frac{(1.96 \sigma_{DW}) / \sqrt{N_{DW}}}{\overline{DW}} \times 100 \quad (54)$$

where  $\sigma_{DW}$  = the standard deviation of the moisture by dry weight,

$N_{DW}$  = the number of moisture samples, and

$\overline{DW}$  = the mean moisture by dry weight.

Similarly, the percentage error in the mean density,  $\epsilon_D$ , is calculated as

$$\epsilon_D = \frac{(1.96 \sigma_D) / \sqrt{N_D}}{\overline{\rho_s}} \times 100 \quad (55)$$

where  $\sigma_D$  = the standard deviation of the density,

$N_D$  = the number of density samples, and

$\overline{\rho_s}$  = the mean soil density.

Assuming that the two errors are independent, the percentage error in the estimate of volumetric moisture content,  $\epsilon_{MVP}$ , is

$$\epsilon_{MVP} = \sqrt{\epsilon_{DW}^2 + \epsilon_D^2} \quad (56)$$

and the actual error in the estimate of volumetric moisture content,  $\epsilon_{MV}$ , becomes

$$\epsilon_{MV} = \frac{\epsilon_{MVP}}{100} \times \theta \quad (57)$$

Then the error in the calculated depth of water,  $\epsilon_G$ , is

$$\epsilon_G = \epsilon_{MV} \times 250 \quad (58)$$

where 250 = the depth of the soil layer (mm).

In a single neutron depth probe measurement of volumetric moisture the three errors which may arise are: a counting error due to the random decay of the source, a vertical location error due to the improper positioning of the probe in the access tube, and a calibration error. The counting error,  $\epsilon_I$ , can be determined from eq. (38). The calibration error,  $\epsilon_c$ , may be considered to be constant at 1.96 times the value of the standard error of the calibration line. In the following calculations  $\epsilon_c$  was taken to be equal to 0.002 moisture volume fraction. The vertical location error,  $\epsilon_{LV}$ , is determined by assuming a positioning error, say  $\pm 5$  mm, then calculating the moisture contents at a distance of  $\pm 5$  mm from the point at which the measurement was made and finding the average absolute value of the difference from the measured value. Thus at any depth  $Z$ ,

$$\epsilon_{LV} = \frac{|\theta_Z - \theta_{Z-5}| + |\theta_Z - \theta_{Z+5}|}{2} \quad (59)$$

where  $\theta_Z$  = the volumetric moisture content at depth Z,  
 $\theta_{Z-5}$  = the volumetric moisture content at depth Z-5,  
 and  
 $\theta_{Z+5}$  = the volumetric moisture content at depth Z+5.

At any single depth the error in the volumetric moisture content is

$$\epsilon_{VM} = \sqrt{\epsilon_I^2 + \epsilon_{LV}^2 + \epsilon_C^2} \quad (60)$$

and the error in the calculated depth of water for that soil layer becomes

$$\epsilon_Z = \epsilon_{VM} \times 100 \quad (61)$$

where 100 = the depth of the soil layer.

For the deepest layer, 1350 to 1400 mm, 100 is replaced by 50.

To find the total error in the calculated depth of water in the entire soil profile,  $\epsilon_{Sm}$ , it is necessary to add the gravimetric and neutron probe components to give

$$\epsilon_{Sm} = \sqrt{\epsilon_G^2 + \sum_{Z=300}^{1400} \epsilon_Z^2} \quad (62)$$

The error in the change of soil moisture at a single site,  $\epsilon_{\Delta Sm}$ , can then be found from

$$\epsilon_{\Delta Sm} = \sqrt{\epsilon_{Sm(1)}^2 + \epsilon_{Sm(2)}^2} \quad (63)$$

where the subscripts (1) and (2) refer to the successive measurements of the soil moisture profile.

This analysis was performed for all measurements at the six sites. The average error in the calculated Sm was 1.80 mm. Included in this amount was an average gravimetric error of 1.40 mm and an error of 1.11 mm in the depth probe measurements. Thus, the gravimetric error accounted for approximately 61 percent of the total error although it applied to less than 18 percent of the soil profile. The two variable errors in the depth probe measurements, the counting and vertical location errors, averaged 0.0024 and 0.0008 moisture volume fraction respectively.

The quantity of most interest to this study is the error in the estimate of  $\Delta Sm$ . Absolute errors are summarized in Table 8 and each is expressed as a percentage of the observed soil moisture change in Table 9. The average absolute error was 2.53 mm, while percentage errors ranged between 12 and 1700 percent, with a median of 34 percent. If a maximum allowable error of 10 percent is specified, actual soil moisture change between measurements

Table 8Summary of absolute errors in  $\Delta S_m$  (mm)

Period	Site 1	Site 2	Site 3	Site 4	Site 5	Site 6
July 1 - 4	3.16	2.19	2.66	2.25	2.33	2.93
4 - 8	2.74	2.38	2.65	2.43	2.24	2.77
9 - 13	2.40	2.32	2.50	2.93	2.33	2.63
14 - 17	2.21	2.07	2.50	2.78	2.38	2.36
18 - 21	2.18	2.16	2.46	2.26	2.84	2.70
22 - 25	2.61	2.12	2.79	3.03	2.69	3.06
Mean	2.55	2.21	2.59	2.61	2.47	2.74

Table 9Summary of percentage errors in  $\Delta S_m$ 

Period	Site 1	Site 2	Site 3	Site 4	Site 5	Site 6
July 1 - 4	44	38	22	49	25	35
4 - 8	105	121	279	1738	51	153
9 - 13	13	16	15	20	12	19
14 - 17	16	98	29	71	16	31
18 - 21	111	13	25	20	62	25
22 - 25	652	18	55	33	94	536

should average 25.3 mm whereas an average absolute value of only 7.2 mm was observed. This means that the sampling period of 4 days was not long enough to accurately measure  $\Delta S_m$  at a single site or to measure differences between sites. Such a low degree of accuracy partially explains the poor correspondence between individual 4-day values of  $(P - \Delta S_m)$  and the corresponding energy balance totals of evapotranspiration.

The error analysis makes it possible to infer optimum sampling intervals. During the 25 days of the experiment  $\Delta S_m$  averaged  $-1.54 \text{ mm day}^{-1}$ . Thus, a basic interval of 17 days was necessary to ensure an error of less than 10 percent at a single site. The interval is not significantly decreased by using a 5-minute counting time. For example, the 5-minute count used at site 5 on July 1 decreased the error by 13 percent. This has the effect of decreasing the basic sampling interval by only 2 days. The improvement is slight because the counting error is only one of three probe errors, the sum of which accounted for less than 40 percent of the total error in a measurement.

The basic interval can be decreased considerably by considering the mean value of  $\Delta S_m$  for all sites. The error in the mean can be calculated by dividing the

average error in  $\Delta S_m$  by the square root of  $(n-1)$ , where  $n$  is the number of sites. This yields a value of 1.13 mm for the present study. Thus the basic interval between measurements should have been 8 days to ensure an error of less than 10 percent in the mean value of  $\Delta S_m$ .

The calculated errors, based on a 95 percent probability level, represent error limits whereby the actual error would not exceed the calculated error in 95 cases out of 100. The probable error, which applies to 50 cases out of 100, is approximately three times smaller than the error limit. Hence, good agreement can be expected between mean values of  $(P - \Delta S_m)$  and energy balance estimates of  $E$  for periods as short as 4 days.

The calculated errors do not completely account for site-to-site variations in soil moisture change. For the six periods the average standard deviation of the soil moisture change was 3.85 mm so that 95 percent of the variation was within 7.55 mm. The average error at a 95 percent probability level at a single site was 2.53 mm, thus accounting for 34 percent of the variation. There are, however, other factors to consider such as differences in infiltration during rainstorms, in rates of water withdrawal by roots, in evaporation at the soil surface and in drainage.

(iv) Evaluation of drainage and its effect on the water balance estimates of evapotranspiration

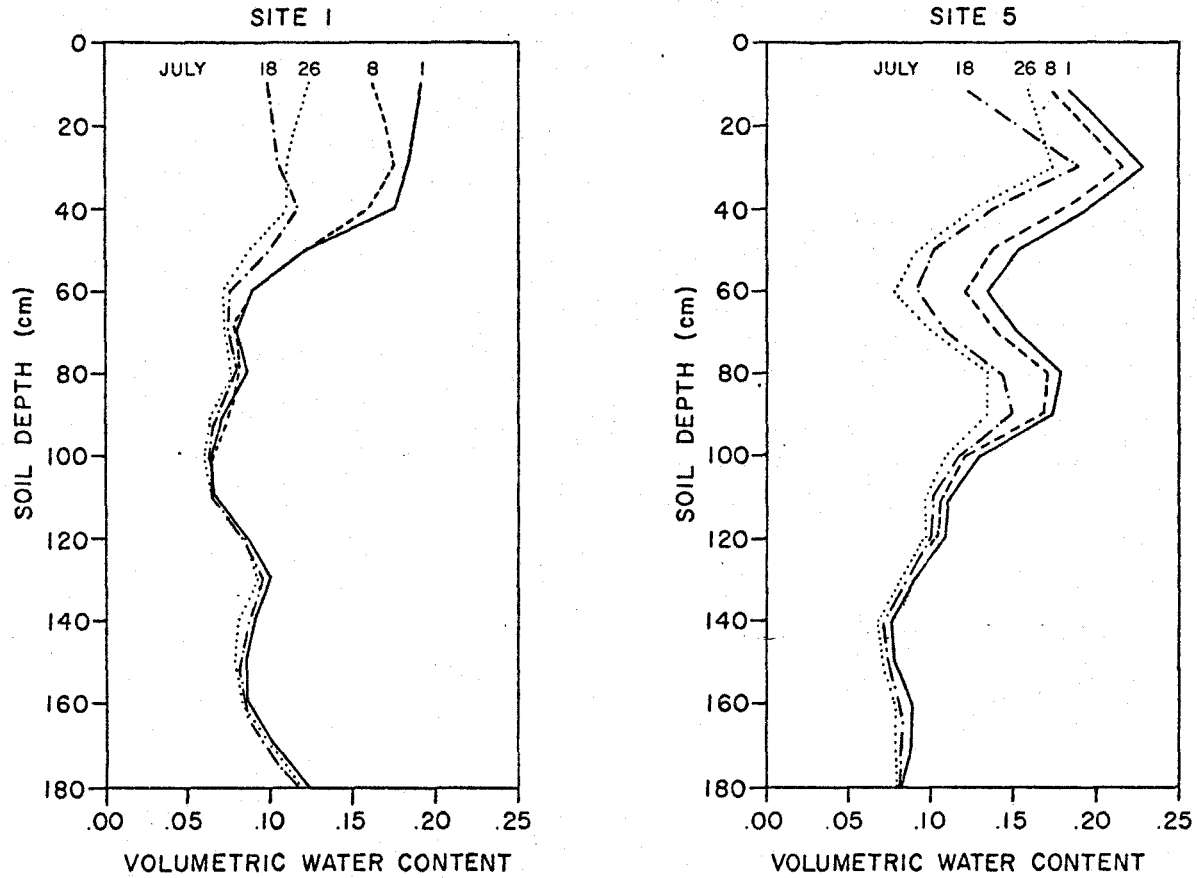
An evaluation of the drainage term,  $V_z$ , in the water balance equation requires a knowledge of the hydraulic gradient and the capillary conductivity. The hydraulic gradient measurements were readily accomplished but considerable difficulty was experienced in determining conductivities.

A summary of the mean hydraulic gradients observed at the six sites is presented in Table 10. At all times a downward water movement was indicated and since the overall mean gradient was 1.02, the drainage was induced primarily by gravity. However, there were consistently large differences between sites. This was not unexpected because there were considerable differences in the shapes of the soil moisture content profiles as can be seen by comparing the profiles for sites 1 and 5 (Fig. 19).

An attempt was made to determine  $k_z$  from eq. (42) using field measurements made at each site after the crop was harvested. Following the suggestion of Rose and Krishnan (1967) the soil surface around each site was covered with sheets of plastic to eliminate the precipitation and evapotranspiration terms in the equation. Attempts to calculate  $k_z$  by this method failed in two

FIGURE 19

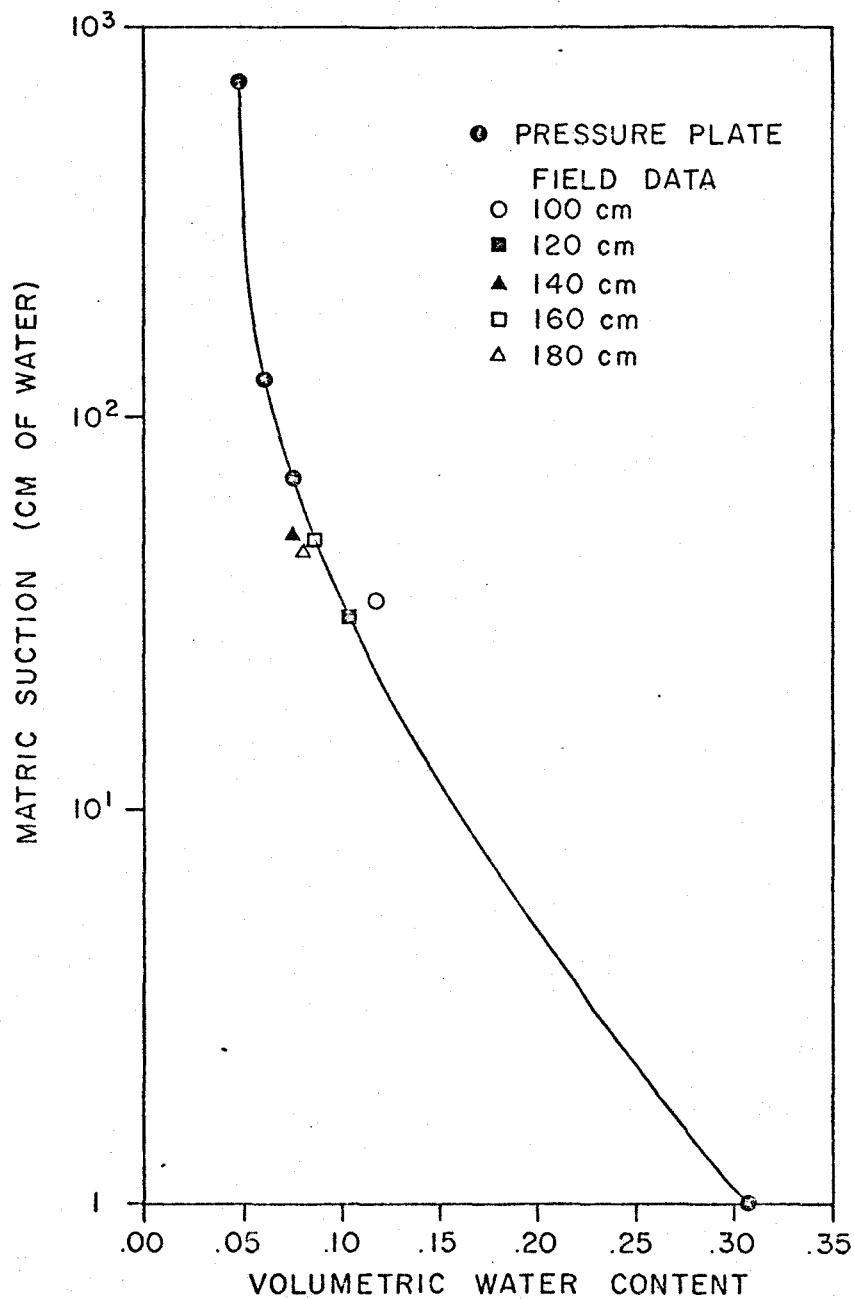
SOIL MOISTURE CONTENT PROFILES AT SITES 1 AND 5 ON SELECTED DAYS DURING JULY 1969.



separate trials. In both cases a soil moisture increase was observed, apparently because some rain water managed to flow under the plastic. An alternate procedure, used by van Bavel et al. (1968b), was also attempted. In this case the measurements from the actual experiment during July, including the energy balance estimates of evapotranspiration, were used to solve eq. (42). However, the individual values of  $(P - \Delta S_m)$  did not always exceed the measured evapotranspiration. This suggested that water was moving upwards into the measurement zone in the soil, whereas the hydraulic gradients consistently indicated conditions favouring drainage. Since this procedure could not be used and since the moisture regimes at the field sites had been altered, it was necessary to determine conductivities using laboratory methods. Two undisturbed soil cores, each 8.0 cm long and with a diameter of 10.5 cm, were extracted vertically at a depth of 140 cm in a pit dug about 4 m east of site 5. Pressure plate apparatus was used to determine the moisture characteristic, and to determine conductivity values.

The moisture characteristic derived from the pressure plate results is shown in Fig. 20 in conjunction with some averaged field data from site 5. There was good agreement between the two sets of data, but the complete field data

FIGURE 20  
MOISTURE CHARACTERISTIC FOR 140 CM  
DEPTH AT SITE 5



indicate that the moisture characteristic changed with depth (Fig. 21) and also changed between sites (Fig. 22). Generalized characteristics for various groups of depths are shown in Fig. 22 and these indicate that the soil was relatively uniform in certain layers at a single site but was heterogeneous between sites.

Table 10

Mean hydraulic gradients at the six sites

Period	Site 1	Site 2	Site 3	Site 4	Site 5	Site 6	Mean
July 1 - 4	1.17	1.32	0.97	0.76	1.07	0.91	1.03
4 - 8	0.96	1.31	0.86	0.70	1.18	1.18	1.03
9 - 13	0.91	1.29	0.95	0.69	1.16	1.09	1.01
14 - 17	0.90	1.22	0.88	0.84	1.17	0.89	0.98
18 - 21	1.01	1.25	0.97	0.68	1.20	1.08	1.03
22 - 25	0.94	1.23	0.92	0.71	1.17	1.17	1.02
Mean	0.98	1.27	0.93	0.73	1.16	1.05	1.02

Capillary conductivities were calculated from the pressure plate outflow data using the method of Gardner (1956). Data from the first pressure increment were discarded because the method has been proven to be inaccurate for wet soil, even when the method is extended to include the effect of

FIGURE 21  
GENERALIZED MOISTURE CHARACTERISTICS FOR  
VARIOUS DEPTHS AT SITE 5

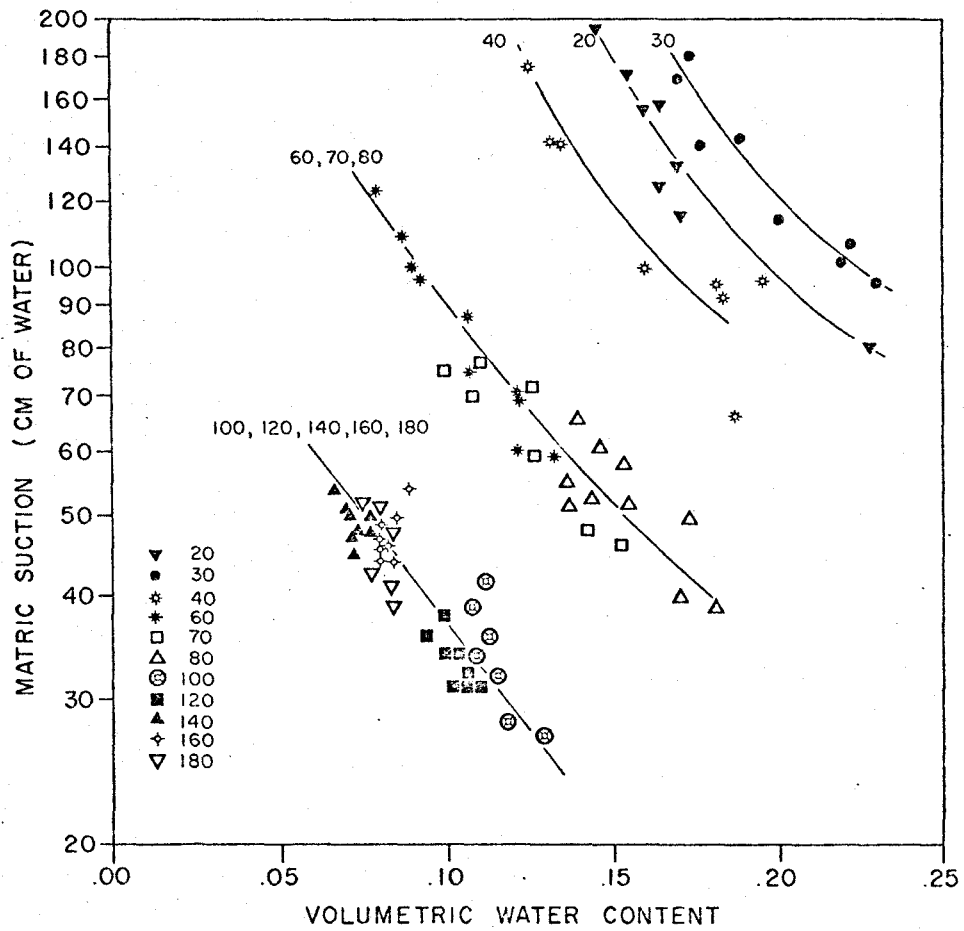


FIGURE 22  
 MOISTURE CHARACTERISTICS AT 120 CM, 140 CM, AND  
 160 CM DEPTHS USING DATA FROM ALL SITES

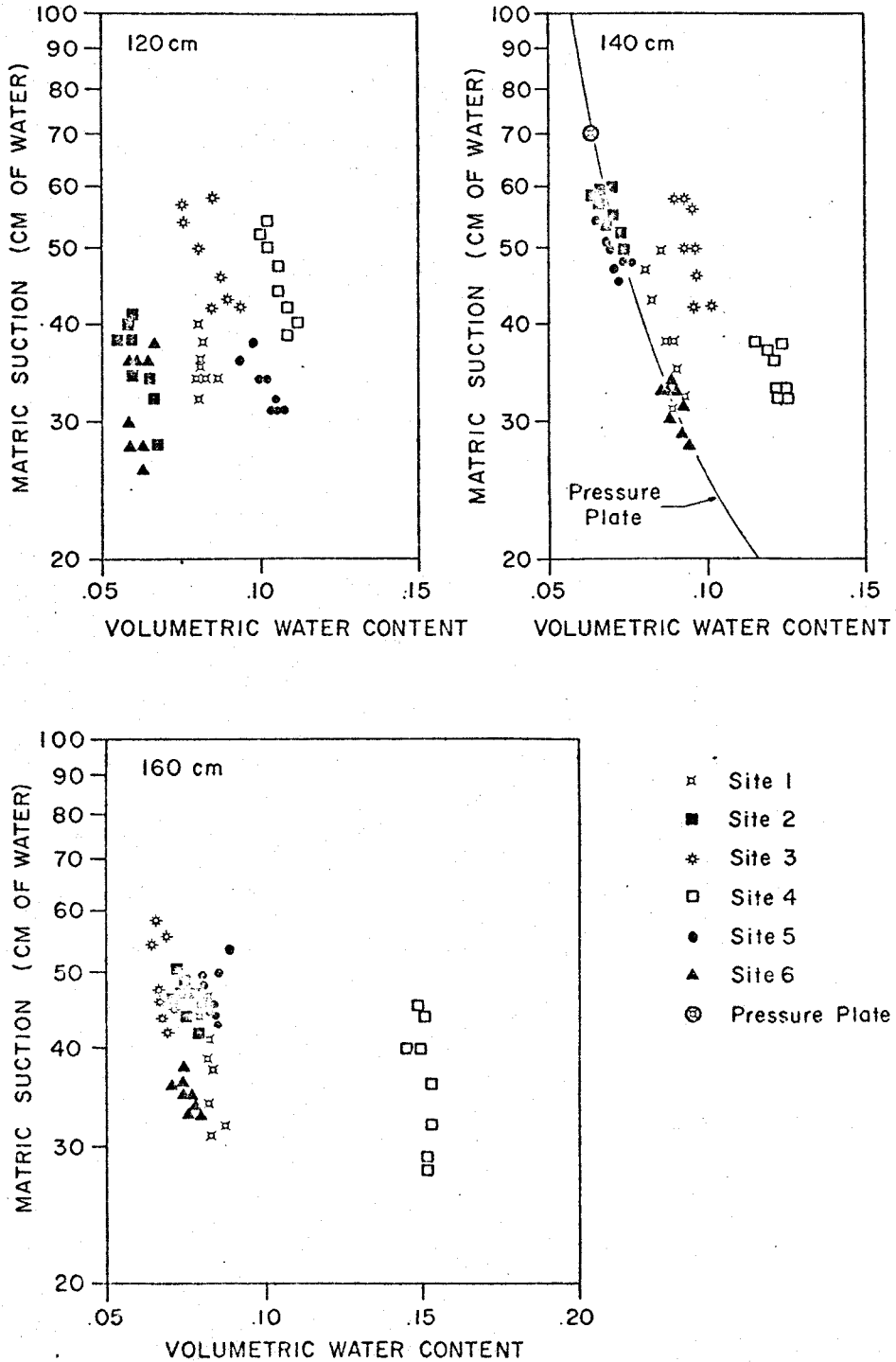


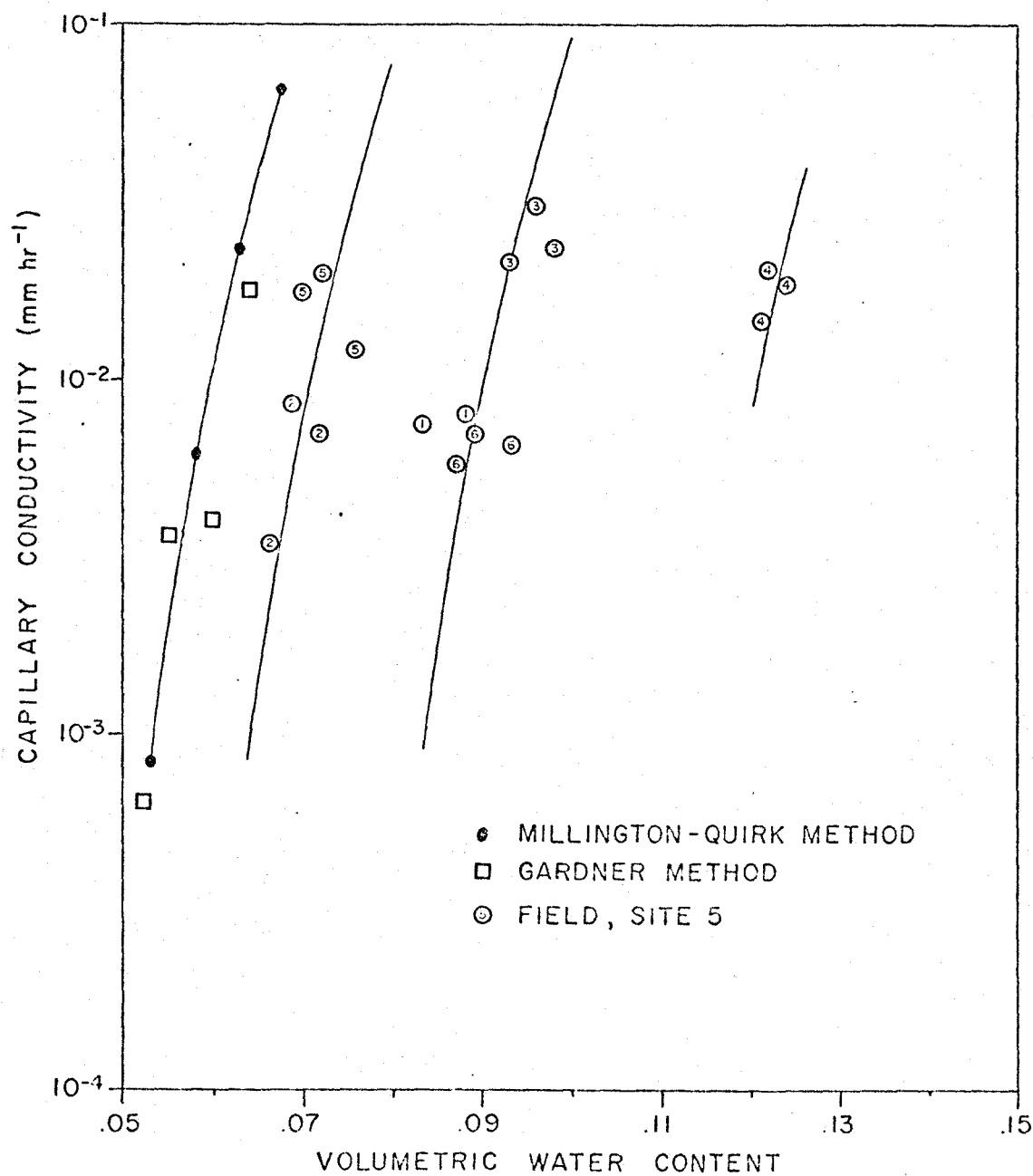
plate impedance (Elrick, 1963). Conductivities were also calculated using the Marshall (1958) and the Millington and Quirk (1959, 1961) equations. As shown in Fig. 23, the Millington and Quirk values agreed well with those determined by the Gardner method, but the Marshall values were two orders of magnitude larger.

The conductivity characteristic derived from the Millington and Quirk method was used to calculate the drainage at each site. These estimates were, however, several orders of magnitude too large and there were considerable differences between sites. The latter feature arose because the moisture contents at the terminal depth ranged from less than 7 percent at the driest site to more than 12 percent at the wettest. Over this range, conductivity values changed by 4 orders of magnitude, with a value of 15 mm per hour at a moisture content of 12 percent. Further testing showed that the results were not improved by applying a matching factor to either the Marshall or the Millington and Quirk conductivity curves. It seems that conductivity characteristics must have been different at the various sites, a feature also noted in the study by van Bavel et al. (1968b).

Conductivities have been determined from the field data, based on the assumption that there was no soil moisture movement at the 80 cm depth as indicated by the

FIGURE 23

CAPILLARY CONDUCTIVITY VALUES FOR THE 140 CM  
DEPTH DETERMINED BY VARIOUS METHODS



hydraulic head profiles at sites 1 and 5. Soil moisture change in the layer 80 - 140 cm was treated as drainage and amounted to 7.63 mm during the 25 days of the study. This represents 9.1 percent of the evapotranspiration estimated by the energy balance method.

Conductivities were calculated from eq. (42) using weekly data so that there would be increased accuracy in estimates of  $\Delta S_m$ . The results of this trial are shown in Fig. 23. The field data fell into three groups. Curves shown were drawn parallel to the Millington and Quirk curve and fitted to the centroid of the points in a given group. There does not seem to be a pattern to the grouping, other than similarity of moisture contents. The points for site 4 are separated from the rest as they also were for the moisture characteristics.

It is evident that the good agreement between E and  $(P - \Delta S_m)$  values, seen in Fig. 17A, would deteriorate if a correction for drainage was applied to the water balance estimates. Such a correction would make the water balance estimates smaller than the corresponding energy balance values.

#### 4. Significance Of Results

This study has shown that the water balance model can produce accurate estimates of evapotranspiration. Estimating drainage has proved difficult in this and in previous studies. Consequently, the model will provide satisfactory results only when the drainage term can be omitted from the water balance equation. The accuracy of the evapotranspiration estimate is partly determined by the error in the measurement of soil moisture storage change. The error analysis presented here provides a method of calculating that error and thereby determining the optimum sampling interval.

## CHAPTER 5

### EVAPOTRANSPIRATION ESTIMATES FROM THE EQUILIBRIUM MODEL

#### 1. Performance in Relation to Available Moisture

Tests were applied to both the hourly and daily equilibrium evapotranspiration estimates to examine the range of conditions over which the model applies.

The hourly values were examined specifically to test the contention that the model applies to a non-saturated atmosphere. Equilibrium estimates were compared with the corresponding energy balance values and there was agreement to within 5 percent of the net heat supply ( $R_n - G$ ) during 100 out of 375 hours. None of these involved saturated air.

The close correspondence between  $LE_{EQ}$  and  $LE$  might be due to very small differences between  $D$  and  $D_0$ , very large values of  $r_a$ , or a combination of these two factors. It will be shown later that the actual and equilibrium evapotranspiration values were in good agreement when there were very small depression gradients between heights of 10 cm and 60 cm above the crop. Thus the condition  $LE_{EQ} \approx LE$  was primarily due to small

wet-bulb depression differences between the 60 cm height and the evapotranspiring surface.

Daily totals of the equilibrium evapotranspiration are plotted against the corresponding energy balance values in Fig. 24. The data fall into three groups according to the prevailing moisture conditions: (1) days when rain occurred, days following a night rain, and days with short periods of reversed sensible heat flux, (2) clear dry days when the crop canopy was open; (3) days on which moisture conditions were between (1) and (2). The results of regression analyses of these groups of data are presented in Table 11.

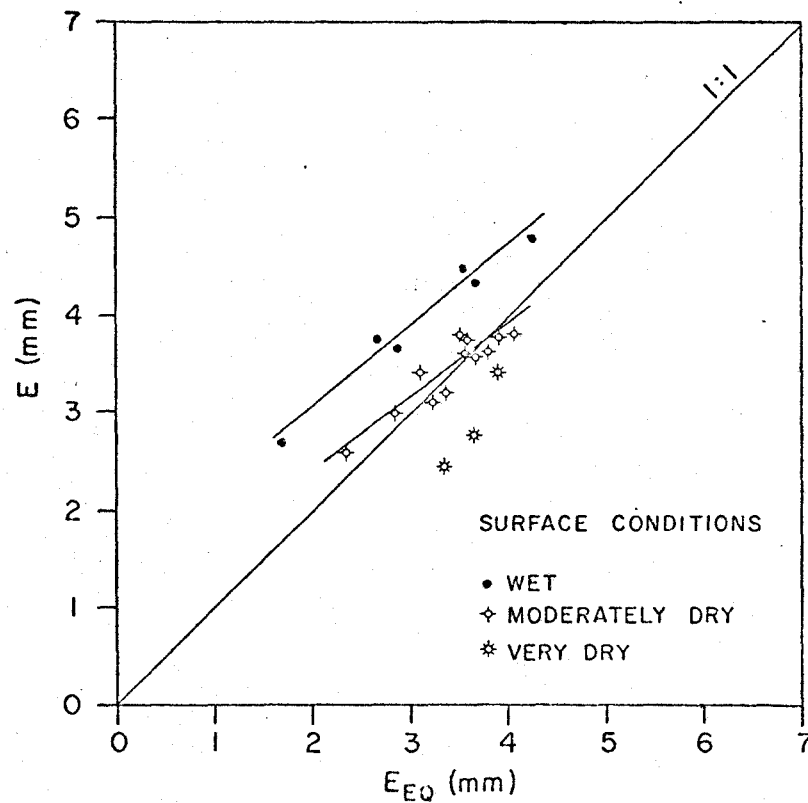
Table 11

Regression and correlation constants for relationships between  $E$  and  $E_{EQ}$  of the form  $E = a + bE_{EQ}$  (mm day<sup>-1</sup>)

<u>Description</u>	<u>a</u>	<u>b</u>	<u>Correlation Coefficient</u>	<u>Standard Error</u>
All days	1.356	0.634	0.65	0.46
Wet surface	1.382	0.829	0.99	0.12
All except wet	1.143	0.635	0.74	0.31
Moderately dry	0.920	0.738	0.95	0.13

FIGURE 24

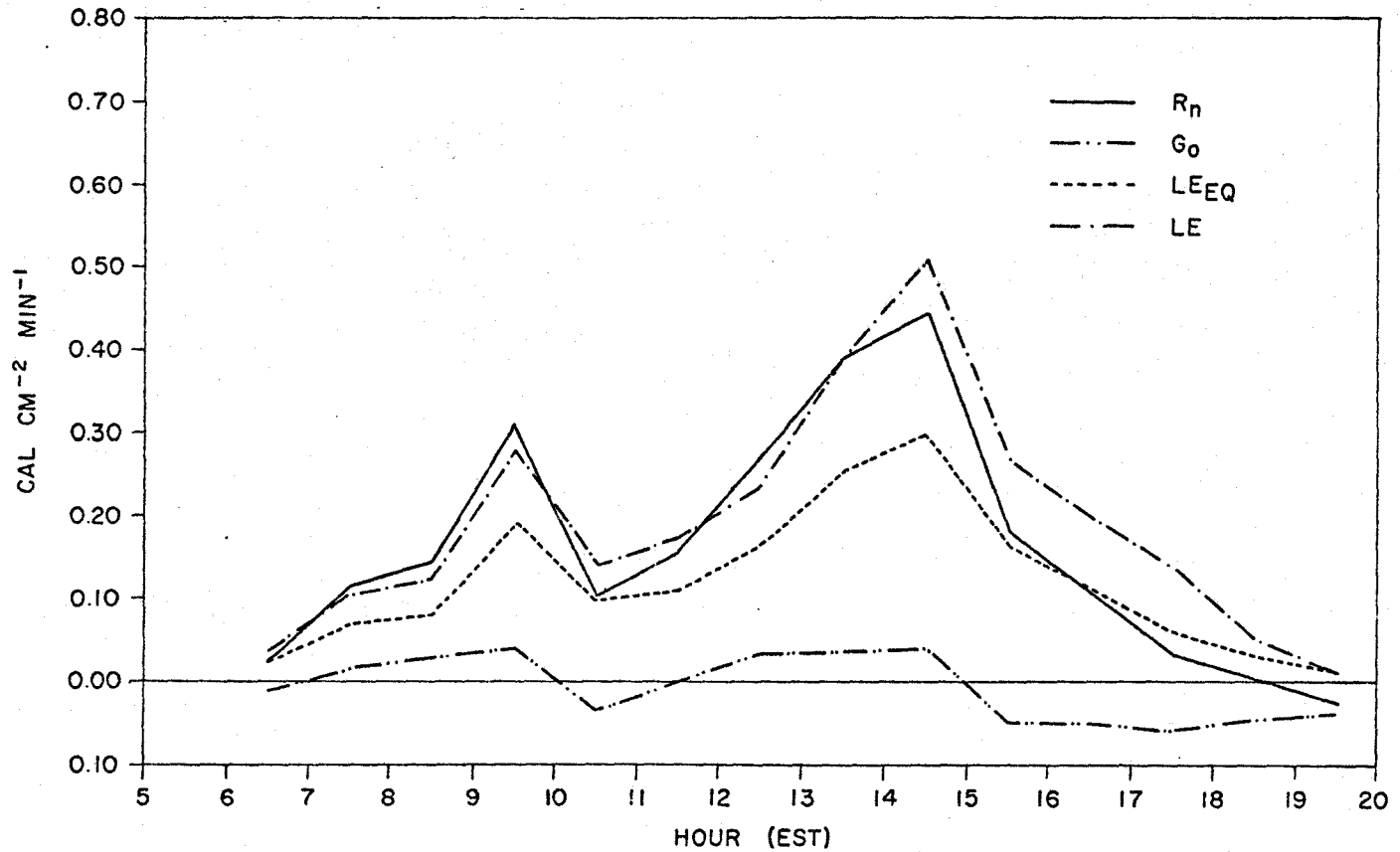
RELATIONSHIP BETWEEN DAILY VALUES OF  $E$   
FROM THE ENERGY BALANCE AND  $E_{EQ}$  FROM  
THE EQUILIBRIUM MODEL



In the first group the actual evapotranspiration was much greater than the equilibrium rate. Such a situation occurred on July 18 (Fig. 25). On days associated with rain, it is probable that the evapotranspiration proceeded at the potential rate. There were also two days, July 22 and 23, on which negative sensible heat flux values were observed for some afternoon hours. During these hours the negative flux did not exceed an absolute value of  $0.10 \text{ cal cm}^{-2} \text{ min}^{-1}$ , but the additional evapotranspiration promoted by this extra heat source was sufficient to cause relatively large discrepancies between measured and predicted daily totals. For general use, similar evapotranspiration models utilize temperature measurements at only one level, so a correction for a negative sensible heat flux cannot be made.

An alternative model can be used for rainy periods. Previous studies have demonstrated that the potential evapotranspiration model (Penman, 1948) produces excellent estimates of the actual vapour flux when the surface is wet or moist. For example, Davies and McCaughey (1968), in an early study at Simcoe, reported good agreement on both an hourly and a daily basis for irrigated perennial ryegrass. The major problem associated with evapotranspiration calculations has been the prediction of the vapour flux on

FIGURE 25  
VARIATION OF ENERGY BALANCE COMPONENTS AND EQUILIBRIUM  
EVAPOTRANSPIRATION ON JULY 18, 1969



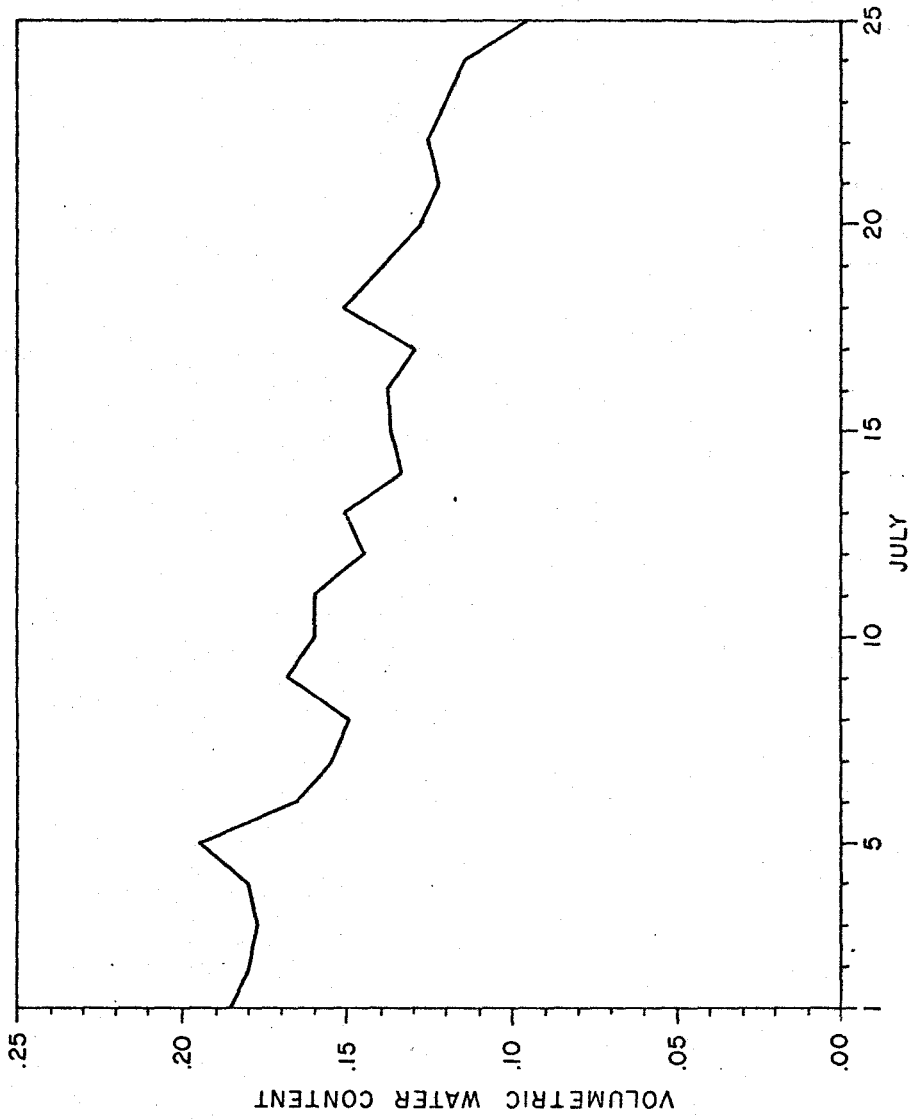
dry days, not wet ones.

A second group of data was composed of three days (July 6, 7, and 8) when the equilibrium model overestimated evapotranspiration. As indicated in Fig. 13, the hourly differences between LE and  $LE_{EQ}$  were consistently large throughout the afternoon on July 6. On the two subsequent days the magnitude of the hourly differences steadily grew, thereby producing steadily increasing overestimates.

Several factors indicate that the rate of water supply to the plant leaves and to the soil surface was severely restricted during the three days. All of these days were clear and sunny and the crop canopy was not yet closed. The Bowen Ratios were considerably higher than the monthly average (Fig. 11) and these were the driest soil conditions experienced in the first nine days of July (Fig. 26). After July 8, this type of deviation from equilibrium evapotranspiration conditions did not occur again, despite similar weather conditions and even drier soil. The growth rate of the crop increased shortly after the dry period and the plants began to shade most of the bare soil. Consequently it appears that the inadequate performance of the model was primarily due to the presence of unshaded bare soil.

The third set of data applied to moderately dry

FIGURE 26  
VARIATION OF SOIL MOISTURE CONTENT IN THE 0-25 CM SURFACE  
LAYER DURING JULY, 1969



days. The points are clustered near the 1:1 line but the actual regression does not go through the origin (Fig. 24). This may be due to a narrow range of data values, but may also be an indication that the model tends to overpredict low values and underpredict high ones. This may be related to air temperature variations and will be discussed later. The standard error of the actual regression line is  $0.12 \text{ mm day}^{-1}$  and this increases to only  $0.21 \text{ mm day}^{-1}$  for a 1:1 relationship. Since the average evapotranspiration on these days was 3.33 mm, the standard error for the  $E = E_{EQ}$  relationship represents only 6 percent of the mean.

The excellent performance of the model for predicting daily totals is a reflection of good agreement between hourly values, and also can be related to the typical diurnal pattern of the differences between LE and  $LE_{EQ}$ . The diurnal trends on July 12 and 15 are shown in Figs. 27 and 28. These days represent contrasting situations since the measured total slightly exceeded the equilibrium total on July 12, whereas on July 15 the situation was reversed. However, the daily patterns of the differences are typical of this group. On sunny days LE was usually greater than  $LE_{EQ}$  until mid-morning when there was a reversal that lasted for a varying length of

FIGURE 27

VARIATION OF ENERGY BALANCE COMPONENTS AND EQUILIBRIUM EVAPOTRANSPIRATION  
ON JULY 12, 1969

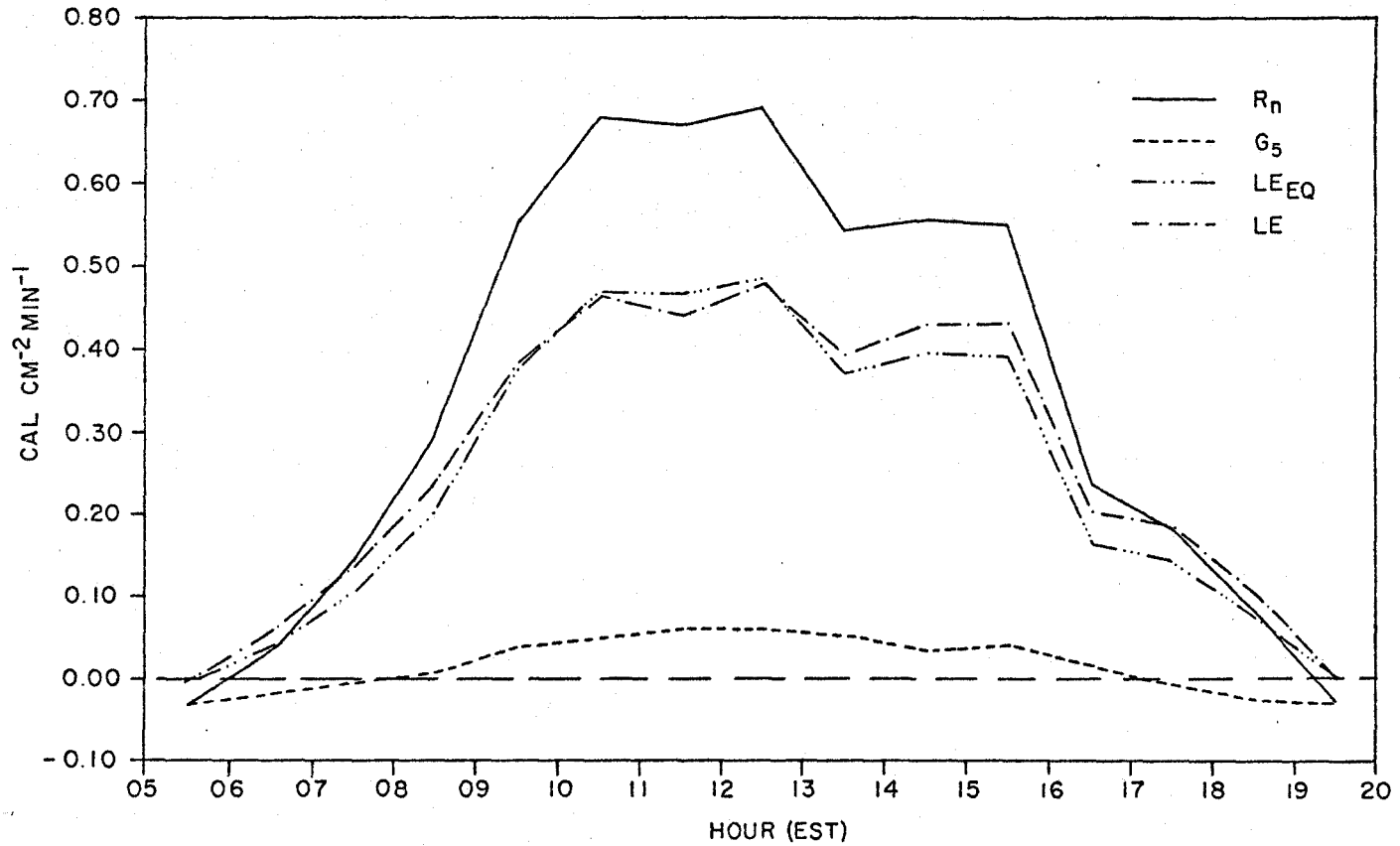
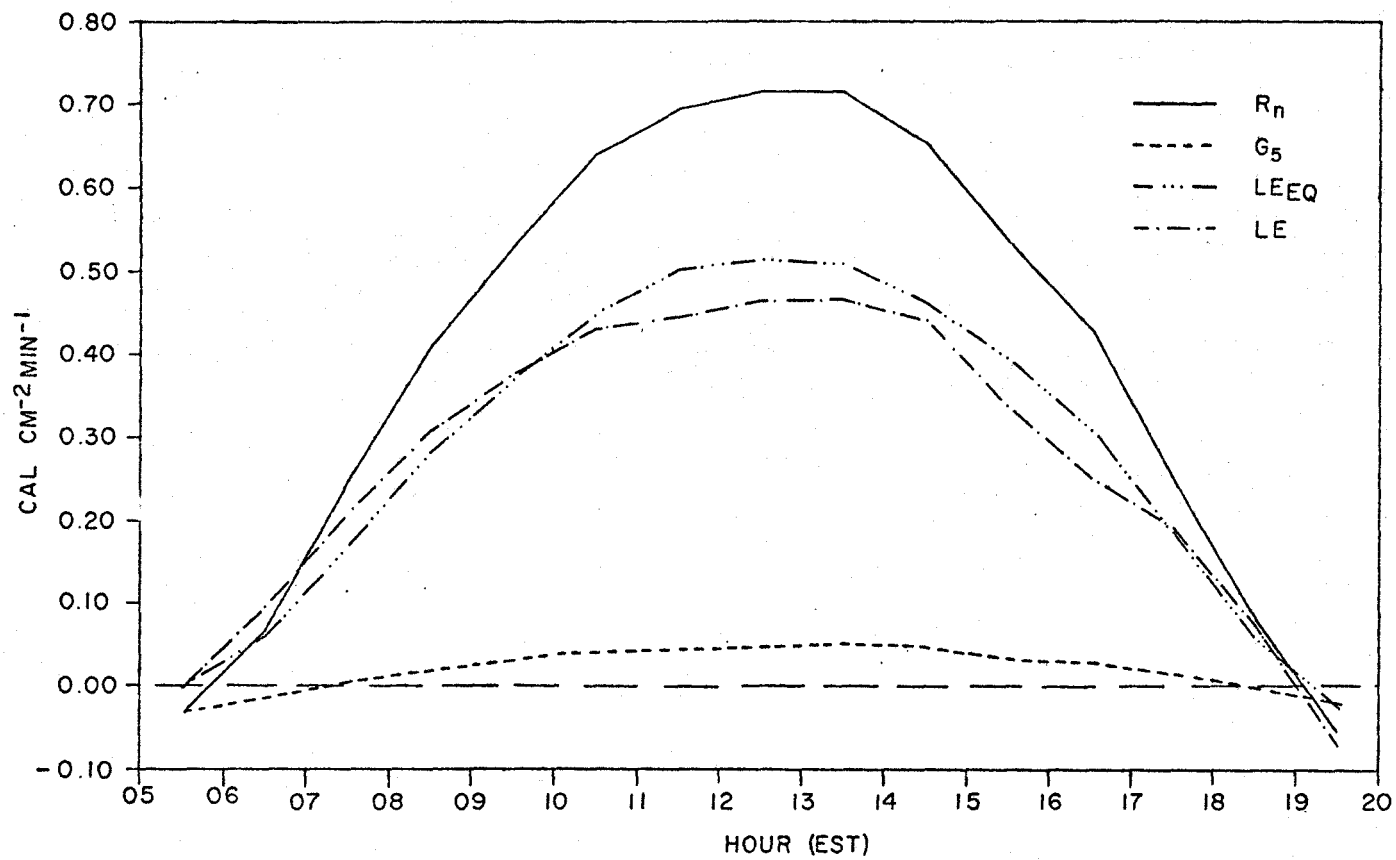


FIGURE 28

VARIATION OF ENERGY BALANCE COMPONENTS AND EQUILIBRIUM EVAPOTRANSPIRATION  
ON JULY 15, 1969



time. By mid- to late-afternoon the situation usually had reverted to the early morning condition again, or else the two values would be nearly equal. On cloudy days the two curves were always close throughout the day.

These patterns are related to available moisture. Under low radiation conditions the rate of water supply, augmented by dew in the mornings, was adequate to maintain an evaporative flux equal to or greater than the equilibrium rate. When there was a demand for a large flow rate in peak radiation conditions the supply became limiting and caused the reversal at mid-day. The peak rate of water supply decreased from the twelfth to the fifteenth, causing the reversal to persist longer at the later date. This is to be expected because the last previous rainfall had occurred on July 10.

## 2. Performance in Relation to Wet-Bulb Depression

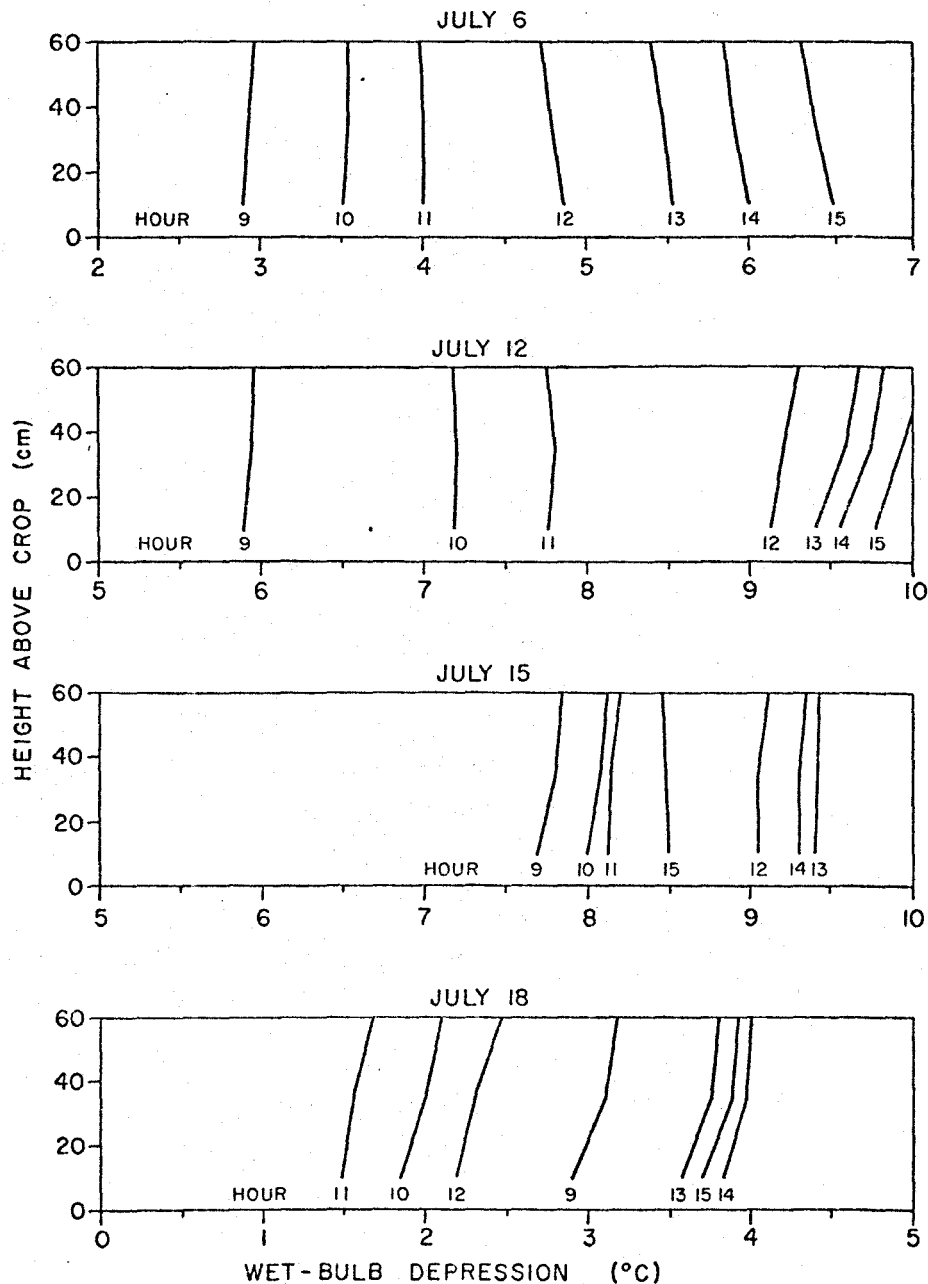
### Profiles

In the equilibrium model it is assumed that the wet-bulb depressions in the overlying air and at the surface are equal. Since the performance of the model was found to be dependent on the prevailing moisture conditions, it can be assumed that the three moisture classes were each associated with a characteristic wet-bulb depression profile.

The observed profiles for the mid-day periods on four days are shown in Fig. 29. A distinct pattern emerges when these profiles are compared to the hourly differences between LE and  $LE_{EQ}$  (Figs. 13, 25, 27, and 28). The depressions increased with height when LE was greater than  $LE_{EQ}$ . This tendency was greatest on the afternoon of July 18 when the surface was wet. In contrast, the gradients were reversed on the afternoon of July 6 when LE was less than  $LE_{EQ}$ . These characteristic profiles persisted throughout the majority of the daylight hours on both the wet and the dry days and so it is not valid to assume that the average depression at the 60 cm height was equal to that at the surface.

On the moderately dry days of July 12 and July 15 there were certain hours near mid-day when  $LE_{EQ}$  exceeded LE. At those times the depressions either increased very slightly between 10 cm and 60 cm, or they were reversed. This mid-day reversal ( $D - D_0 < 0$ ) tended to cancel the effect of the positive gradients ( $D - D_0 > 0$ ) which occurred during the early morning and late afternoon hours. As a result, there was little difference between the average wet-bulb depression in the overlying air and that at the surface, thereby producing excellent agreement between the daily values of LE and  $LE_{EQ}$ .

FIGURE 29  
 WET-BULB DEPRESSION PROFILES ON FOUR DAYS  
 DURING JULY 1969



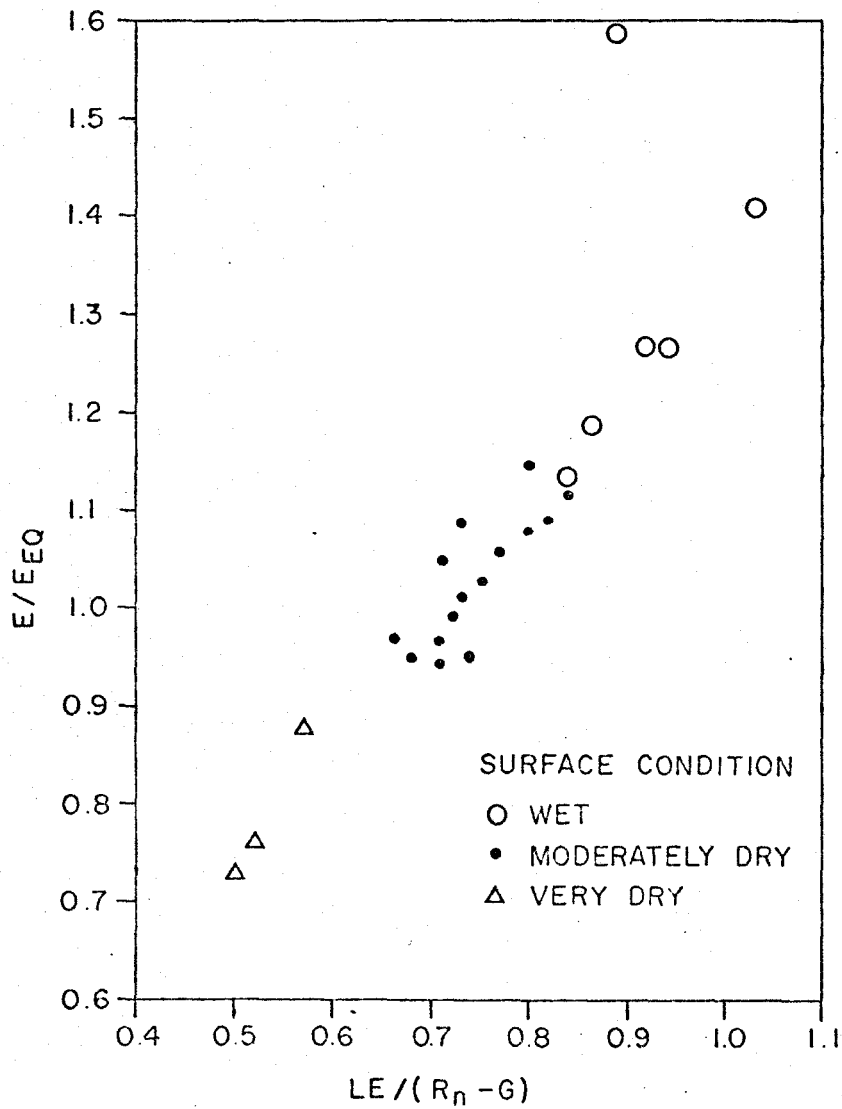
### 3. Moisture and Temperature Limits

The equilibrium model represents a response to particular environmental conditions and it is worthwhile to define precisely those conditions in which it can be used. The two factors to consider are surface moisture conditions and air temperature.

An indirect measure of the surface moisture condition is the ratio  $LE/(R_n - G)$ . When the moisture stress is low the proportion of available energy used for evapotranspiration will be high. In the case of potential evapotranspiration, Davies and McCaughey (1968) found that 86 percent of the available energy was used for this process on a daily basis. This value can be used for comparison in the present study.

Fig. 30 shows a plot of the ratio  $E/E_{EQ}$  against  $LE/(R_n - G)$  using daily totals with the data separated according to the moisture conditions specified earlier. The lowest value of the ratio  $LE/(R_n - G)$  during wet conditions was 0.84 which corresponds closely with the value of Davies and McCaughey. On the three very dry days the ratio  $LE/(R_n - G)$  did not exceed 0.57. For these two conditions  $LE_{EQ}$  differed from  $LE$  by at least 12 percent. On the moderately dry days  $LE/(R_n - G)$  ranged between 0.66 and 0.84. All values greater than

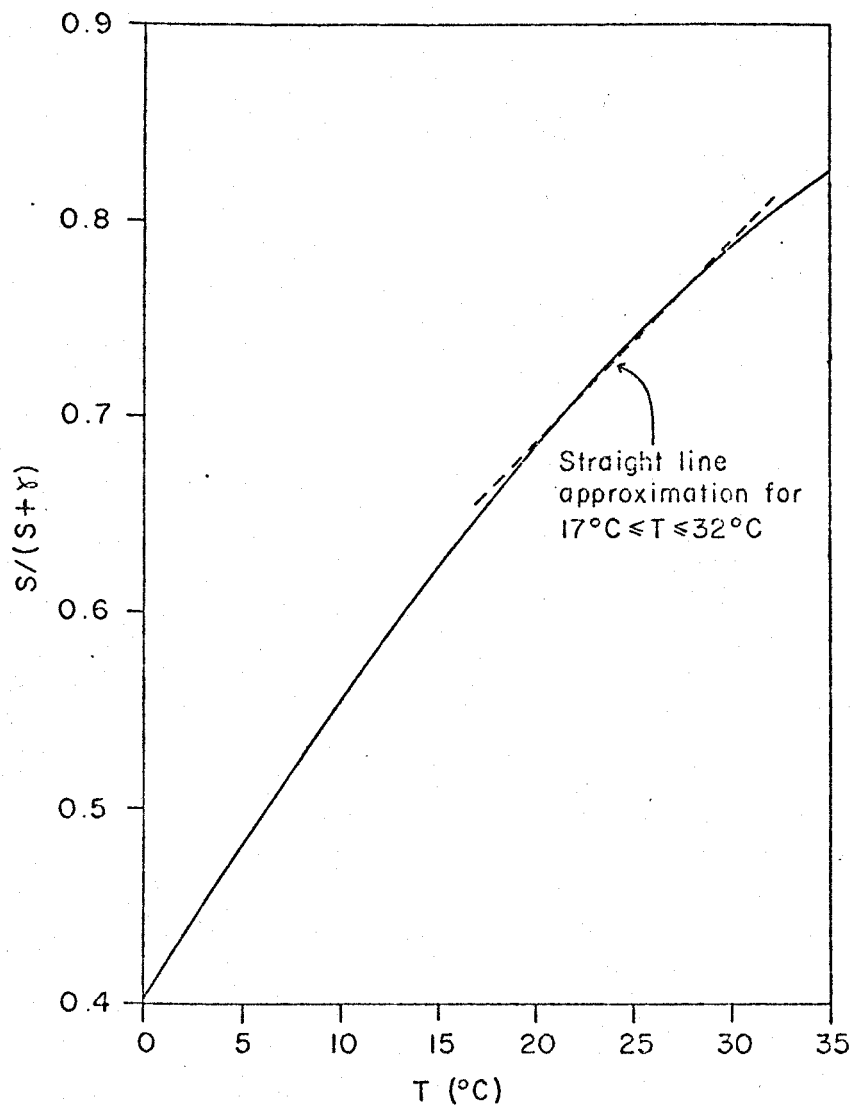
FIGURE 30  
RELATIONSHIP BETWEEN THE RATIO  $E/E_{EQ}$   
AND THE RATIO  $LE/(R_n-G)$  FOR DAILY  
PERIODS



0.80 applied to days when  $(R_n - G)$  was small. Consequently one might assume that the values of 0.65 and 0.80 define the limits within which the model is generally applicable.

It is apparent in eq. (36) that the proportion of the available energy used for equilibrium evapotranspiration is determined by the value of  $S/(S + \gamma)$ , and is thus dependent on air temperature. The variation of this factor with temperature is shown in Fig. 31 from which three facts emerge. Firstly, temperature values of  $17^{\circ}\text{C}$  and  $32^{\circ}\text{C}$  correspond to  $LE/(R_n - G)$  values of 0.65 and 0.80, respectively. Thus there are thermal limits to the model's applicability. Secondly, although the proportionality factor is temperature dependent and air temperature changes with height, the actual height of the temperature measurement is not critical. Values of  $S$  change slowly in the  $17^{\circ} - 32^{\circ}\text{C}$  temperature range, and changes in  $S/(S + \gamma)$  are even more conservative: a temperature change of  $1^{\circ}\text{C}$  alters the ratio by only 0.01. Under the conditions of this experiment it is probable that only a slight difference in predicted evapotranspiration values would have been found if the temperatures had been measured at the standard screen height of 1.5 m. Thirdly, the value of  $S/(S + \gamma)$  can be calculated with sufficient accuracy by a straight line approximation to

FIGURE 31  
VARIATION OF THE FACTOR  $S/(S+\gamma)$  WITH  
TEMPERATURE



the curve shown in Fig. 31. The equation of the straight line in the temperature range 17° - 32°C is

$$\frac{S}{S + \gamma} = 0.483 + 0.0102 T \quad (64)$$

which has a standard error of only 0.003. This equation provides a simple and accurate method of calculating the proportionality factor and permits quick estimation of the equilibrium evapotranspiration.

There have been two previous tests of the equilibrium model. Pruitt and Lourence (1968) expected that equilibrium conditions would apply when there was dew lying on the surface because the air layer near the ground would be nearly saturated with water vapour. The equilibrium predictions did not agree with observed values so they arbitrarily changed the proportionality factor from  $S/(S + \gamma)$  to  $S/(S + 2\gamma)$ . However, the original derivation of the factor is precise and there is no physical reason to justify the alteration. Denmead and McIlroy (1970) compared hourly values of equilibrium evapotranspiration with measured values. The data exhibited a moderate degree of scatter and the model produced underestimates at high evapotranspiration rates. Much better agreement was found in the present experiment because the equilibrium model produced both underestimates and overestimates

during the daylight period, and these offset each other in the daily total. Underestimates at high evapotranspiration rates were also noted for the daily values in this study and it has been shown that these discrepancies are a response to either moisture or temperature conditions. The present research indicates that underestimates will be produced if the ratio  $LE/(R_n - G)$  exceeds a value of 0.73 or if air temperatures are lower than  $25^{\circ}\text{C}$ .

#### 4. Significance of Results

This study shows that the equilibrium evapotranspiration model can be applied to a non-saturated atmosphere when evapotranspiration proceeds at less than the potential rate and when the water supply to the vegetation is not severely restricted. The model provides accurate daily estimates when used within specified moisture and temperature limits. Consequently, it is the only physical evapotranspiration model utilizing atmospheric measurements which has proven to be operational for dry vegetated surfaces.

## CHAPTER 6

### SUMMARY AND CONCLUSIONS

#### 1. The Water Balance Model

The water balance model was employed to estimate evapotranspiration for daily periods at a single site and for 4-day periods at six sites, all measurements being made in a corn field growing in sandy loam soil at Simcoe, Ontario. Precipitation was monitored at three sites along the edges of the field and soil moisture storage change was measured using neutron moderation and gravimetric techniques. Surface runoff and lateral subsurface flow of soil water were considered to be negligible. Attempts were made to determine the water drainage using methods described in previous studies, but these were not successful. Although no estimate of drainage could be derived for the individual measuring periods a value for the total experimental period was obtained.

Daily estimates of evapotranspiration from the water balance model compared poorly to those calculated from the energy budget. Estimates for 4-day periods compared well except for one case when intensive rainfall led to considerable surface runoff. An analysis of potential errors in the

calculation of soil moisture storage change allowed the formulation of restraints for using the water balance model to estimate evapotranspiration. Under the environmental conditions of this experiment the time interval between measurements necessary to achieve reliable estimates proved to be 17 days for measurements at a single site and 8 days for the averaged values from six sites. Satisfactory results were achieved using a 4-day period between measurements, but there is less certainty of good performance for this shorter interval.

Several conclusions can be drawn regarding the accuracy of the water balance model for estimating evapotranspiration. The approach is not suitable for daily periods. Weekly estimates are reliable providing the change in soil moisture storage is of sufficient magnitude to reduce measurement errors to acceptable levels. If evapotranspiration is small or there is a large precipitation input over the measurement period, the time interval between measurements must be increased. Surface runoff cannot be ignored for intense rainfalls, even in very porous soils such as those at Simcoe. It is also necessary to replicate experimental sites to diminish the effects of soil heterogeneity; the desirable number of sites will be determined by the spatial variation in the soil's physical properties.

## 2. The Equilibrium Model

The only variables which determine the evapotranspiration estimate derived from the equilibrium model are air temperature and available heat energy. This study shows that the model can be used in certain non-saturated atmospheric conditions as well as in a saturated atmosphere. The accuracy of the equilibrium evapotranspiration estimates was affected by surface moisture conditions. On moderately dry days it gave estimates which were within 6 percent of energy balance calculations. This good agreement was related to a diurnal pattern where underestimates in the morning and late-afternoon were compensated by overestimates at mid-day. The results are in good agreement with those of Denmead and McIlroy (1970). The better response of the model in this study is due to the use of daily rather than hourly periods. Predictions were not good for wet and for very dry conditions. In wet conditions the prediction was too low and in dry conditions too high.

The evidence in this study shows that the model is applicable for mean daily air temperatures between 17° and 32°C, and is insensitive to small temperature changes so that the exact height of the measurement is not important. The factor  $S/(S + \gamma)$  can be calculated accurately within the designated temperature range from a simple linear equation with air temperature as the independent variable. This gives a very simple calculation of evapotranspiration.

This study indicates that it should be possible to combine the use of a potential evapotranspiration model and the equilibrium model to predict daily totals of evapotranspiration for a variety of surface conditions. There may be certain transition situations when neither model is entirely valid, but this is a problem which could be investigated in future research. Such a combination would be preferable to the water balance model. The measurements are simpler than those required for the water balance and accurate estimates can be made for a much shorter time period.

#### REFERENCES

- Bell, J. P., and C. W. O. Eeles, 1967: Neutron random counting error in terms of soil moisture for non-linear calibration curves. Soil Sci., 103, 1-3.
- Black, J. D. F., and P. D. Mitchell, 1968: Soil moisture estimation by the neutron scattering method in Britain. J. Hydrol., 4, 254-263.
- Black, T. A., W. R. Gardner and C. B. Tanner, 1970: Water storage and drainage under a row crop on a sandy soil. Agron. J., 22, 48-51.
- Blackwell, M. J., and J. B. Tyldesley, 1965: Measurement of natural evaporation: comparison of gravimetric and aerodynamic methods. Methodology of Plant Ecology, Proc. Montpellier Symp., UNESCO, 141-148.
- Bowen, I. S., 1926: The ratio of heat-losses by conduction and by evaporation from any water surface. Phys. Rev., 27, 779-789.
- Bowman, D. H., and K. M. King, 1965: Determination of evapotranspiration using the neutron scattering method. Can. J. Soil Sci., 45, 117-126.

- Brunt, D., 1934: Physical and Dynamical Meteorology.  
Cambridge University Press, 412 pp.
- Cook, N. H., and E. Rabinowicz, 1963: Physical Measurement and Analysis. Adison-Wesley Pub. Co., 312 pp.
- Davies, J. A., and J. H. McCaughey, 1968: Potential evapotranspiration at Simcoe, Southern Ontario. Arch. Meteor. Geoph. Biokl., B, 16, 391-417.
- Denmead, O. T., and I. C. McIlroy, 1970: Measurements of non-potential evaporation from wheat. Agr. Meteor., 7, 285-302.
- Dilley, A. C., 1968: On the computer calculation of vapor pressure and specific humidity gradients from psychrometric data. J. Appl. Meteor., 7, 717-719.
- Dyer, A. J., 1963: The adjustment of profiles and eddy fluxes. Quart. J. Roy. Meteor. Soc., 89, 276-280.
- \_\_\_\_\_, 1967: The turbulent transport of heat and water vapor in an unstable atmosphere. Quart. J. Roy. Meteor. Soc., 93, 501-508.
- Elrick, D. E., 1963: Unsaturated flow properties of soils. Aust. J. Soil Res., 1, 1-8.
- Fuchs, M., and C. B. Tanner, 1968: Calibration and field test of soil heat flux plates. Soil Sci. Soc. Amer. Proc., 32, 326-328.

\_\_\_\_\_, \_\_\_\_\_, G. W. Thurtell and T. A. Black, 1969: Evaporation from drying surfaces by the combination method. Agron. J., 61, 22-26.

Gardner, W. R., 1956: Calculation of capillary conductivity from pressure plate outflow data. Soil Sci. Soc. Amer. Proc., 20, 317-320.

Goff, J. A., and S. Gratch, 1946: Low pressure properties of water from -160 to 212°F. Trans. Am. Soc. Heat. Vent. Eng., 52, 95-121.

Hewlett, J. D., J. E. Douglass and J. L. Clutter, 1964: Instrumental and soil moisture variance using the neutron-scattering method. Soil Sci., 97, 19-24.

Holmes, J. W., S. A. Taylor and S. J. Richards, 1967: Measurement of soil water. Agronomy, 11, 285-303.

Jackson, R. D., R. J. Reginato and C. H. M. van Bavel, 1965: Comparison of measured and calculated hydraulic conductivities of unsaturated soils. Water Resources Res., 1, 375-380.

Knoerr, K. R. 1965: Contrasts in energy balances between individual leaves and vegetated surfaces. Proc. Ann. Tech. Meeting Inst. Environ. Sci., 615-623.

- Kunze, R. J., G. Uehara and K. Graham, 1968: Factors important in the calculation of hydraulic conductivity. Soil Sci. Soc. Amer. Proc., 32, 760-765.
- Lemon, E. R., 1960: Photosynthesis under field conditions. II. An aerodynamic method for determining the turbulent carbon dioxide exchange between the atmosphere and a corn field. Agron. J., 52, 697-703.
- Lettau, H. H., 1959: A Review of Research Problems in Micrometeorology. Dept. of Meteor., Univ. of Wisconsin, Final Rpt., Contract DA-36-039-5C-80063.
- Lourence, F. J., and W. P. Pruitt, 1969: A psychrometer system for micrometeorology profile determination. J. Appl. Meteor., 8, 492-498.
- Luebs, R. E., M. J. Brown and A. E. Laag, 1968: Determining water content of different soils by the neutron method. Soil Sci., 106, 207-212.
- Marshall, T. J., 1958: A relation between permeability and size distribution of pores. J. Soil Sci., 9, 1-8.
- Millington, R. J., and J. P. Quirk, 1959: Permeability of porous media. Nature, 183, 387-388.
- \_\_\_\_\_, and \_\_\_\_\_, 1961: Permeability of porous solids. Trans. Faraday Soc., 57, 1200-1207.

- Monteith, J. L., 1965: Evaporation and environment. Symp. Soc. Expt. Biol., 19, 205-234.
- Mukammal, E. I., K. M. King and H. F. Cork, 1966: Comparison of aerodynamic and energy budget techniques in estimating evapotranspiration from a cornfield. Arch. Meteor. Geoph. Biokl., B, 14, 384-395.
- Penman, H. L., 1948: Natural evaporation from open water, bare soil and grass. Proc. Roy. Soc. London, A, 193, 120-145.
- \_\_\_\_\_, 1956: Evaporation: an introductory survey. Netherlands J. Agr. Sci., 4, 9-29.
- \_\_\_\_\_, D. E. Angus and C. H. M. van Bavel, 1967: Microclimatic factors affecting evaporation and transpiration. Amer. Soc. Agron. Mono., 11, 483-505.
- Pierpoint, G., 1966: Measuring surface soil moisture with the neutron depth probe and a surface shield. Soil Sci., 101, 189-192.
- Priestly, C. H. B., 1959: Turbulent Transfer in the Lower Atmosphere. Univ. Chicago Press, 130 pp.
- Pruitt, W. O., and F. J. Lourence, 1968: Correlation of climatological data with water requirements of crops. Water Sci. and Eng. Papers, 9001, Univ. of California.

- Richards, L. A., 1949: Methods of measuring soil moisture tension. Soil Sci., 68, 95-112.
- Rose, C. W., W. R. Stern and J. E. Drummond, 1965: Determination of hydraulic conductivity as a function of depth and water content for soil in situ. Aust. J. Soil Res., 3, 1-9.
- \_\_\_\_\_, and A. Krishnan, 1967: A method of determining hydraulic conductivity characteristics for non-swelling soils in situ, and of calculating evaporation from bare soil. Soil Sci., 103, 369-373.
- Rouse, W. R., 1970: Effects of soil water movement on actual evapotranspiration estimated from the soil moisture budget. Can. J. Soil Sci., 50, 409-418.
- Slatyer, R. O., and I. C. McIlroy, 1961: Practical Microclimatology, CSIRO, Melbourne, Australia, 310 pp.
- Swinbank, W. C., and A. J. Dyer, 1967: An experimental study in micrometeorology. Quart. J. Roy. Meteor. Soc., 93, 494-500.
- Tanner, C. B., 1960a: A simple aero-heat budget method for determining daily evapotranspiration. Trans. VII Int. Cong. Soil Sci., 1, 203-209.

- \_\_\_\_\_, 1960b: Energy balance approach to evapotranspiration from crops. Soil Sci. Soc. Amer. Proc., 24, 1-9.
- \_\_\_\_\_, and M. Fuchs, 1968: Evaporation from unsaturated surfaces: a generalized combination method. J. Geoph. Res., 73, 1299-1304.
- Tetens, O., 1930: Uber einige meteorologische Begriffe. Z. Geophys., 6, 297-309.
- van Bavel, C. H. M., 1966: Evaporation and Energy Balance of Alfalfa. Report No. 381, U. S. Dept. Agr., Phoenix, Arizona.
- \_\_\_\_\_, K. J. Brust and G. B. Strik, 1968a: Hydraulic properties of a clay loam soil and the field measurement of water uptake by roots: II. The water balance of the root zone. Soil Sci. Soc. Amer. Proc., 32, 317-321.
- \_\_\_\_\_, G. B. Stirk and K. J. Brust, 1968b: Hydraulic properties of a clay loam soil and the field measurement of water uptake by roots: I. Interpretation of water content and pressure profiles. Soil Sci. Soc. Am. Proc., 32, 310-316.
- van Wijk, W. R., 1965: Soil microclimate, its creation, observation and modification. Meteor. Mono., 6, 59-73.

Yocum, C. S., L. H. Allen and E. R. Lemon, 1964: Photo-  
synthesis under field conditions. VI. Solar radia-  
tion balance and photosynthetic efficiency. Agron.  
J., 56, 249-253.